Relativistic bound-state problem in the light-front Yukawa model

Stanisław Głazek, Avaroth Harindranath, Stephen Pinsky, Junko Shigemitsu, and Kenneth Wilson
Physics Department, The Ohio State University, Columbus, Ohio 43210
(Received 8 June 1992)

We study the renormalization problem on the light front for the two-fermion bound state in the (3+1)-dimensional Yukawa model, working within the lowest-order Tamm-Dancoff approximation. In addition to traditional mass and wave-function renormalization, new types of counterterms are required. These are nonlocal and involve arbitrary functions of the longitudinal momenta. Their appearance is consistent with general power-counting arguments on the light front. We estimate the "arbitrary function" in two ways: (1) by using perturbation theory as a guide and (2) by considering the asymptotic large transverse momentum behavior of the kernel in the bound-state equations. The latter method, as it is currently implemented, is applicable only to the helicity-zero sector of the theory. Because of triviality, in the Yukawa model one must retain a finite cutoff Λ in order to have a nonvanishing renormalized coupling. For the range of renormalized couplings (and cutoffs) allowed by triviality, one finds that the perturbative counterterm does a good job in eliminating cutoff dependence in the low-energy spectrum (masses $\ll\Lambda$).

PACS number(s): 11.10.Gh, 11.10.Ef, 11.10.St, 11.15.Tk

I. INTRODUCTION

Most of our intuitions about bound states in quantum mechanics come from solving Hamiltonians. A variety of methods exist in quantum mechanics to handle Hamiltonians. One would like to apply Hamiltonian methods also to study relativistic systems. In fact, such an attempt has a long history, for example, the Tamm-Dancoff method [1,2] in equal-time field theory in the early 1950s. The equal-time Tamm-Dancoff method was eventually abandoned due to severe ultraviolet problems.

What are the major obstacles encountered in trying to solve relativistic Hamiltonians? First of all, the Hamiltonians of equal-time field theory contain vertices which cause particle creation from the vacuum state. Thus, Hamiltonian diagonalization leads to vacuum divergences. In perturbation theory one can avoid vacuum diagrams but in nonperturbative methods one has to deal with them. Moreover, the vacuum state in equal-time field theory is thought to be quite complex and responsible for many nontrivial phenomena. One must solve for the vacuum state of the Hamiltonian of equal-time field theory before proceeding to calculate the rest of the spectra. A second obstacle arises from truncations which are unavoidable in any practical calculational scheme. In relativistic field theory any physical state is a superposition of an infinite number of bare multiparticle states. In practice one truncates this number (Tamm-Dancoff truncation). Even after the particle number truncation there are still, in general, an infinite set of energy scales which get coupled via the interactions. In practice, one can introduce momentum cutoffs to regulate the theory. The introduction of particle number truncation and momentum cutoffs produces violations of Lorentz invariance. One may try to recover Lorentz invariance by introducing noncovariant counterterms. This is generally considered to be a very unpleasant situation.

The light-front Tamm-Dancoff (LFTD) method was proposed [3] recently to overcome some of the problems in the equal-time Tamm-Dancoff method. A related approach is discretized light-cone quantization (DLCQ) proposed by Pauli and Brodsky [4]. The LFTD method is the Tamm-Dancoff truncation of light-front quantum field theory [5]. In the light-front formulation longitudinal momentum is either positive or zero. One may introduce a longitudinal momentum cutoff ϵ and in the presence of nonzero ϵ all troublesome vacuum diagrams simply disappear and the bare vacuum state becomes an eigenstate of the Hamiltonian. One can also introduce a transverse momentum cutoff Λ to regulate ultraviolet divergences. Note that particle truncation and momentum cutoffs spoil Lorentz symmetries. One has to remove the cutoff dependence from the observables and recover the lost Lorentz symmetries. We have avoided the original vacuum problem but now the construction of the proper Hamiltonian is a nontrivial renormalization problem.

How does one proceed with the renormalization problem of Hamiltonians? Even when one studies relatively simple systems the analysis gets rather involved [6–8]. For the light-front field theory there is a proliferation of possible terms in the Hamiltonian based on power counting (see Appendix A). The source of this is the existence of two different dimensional variables, transverse distance $x_\perp$ and longitudinal distance x^-, which makes nonlocal counterterms inevitable in the renormalization of light-front Hamiltonians in any practical schemes. As a starting point one may take just the canonical Hamiltonian. For a Tamm-Dancoff calculation even in one space and one time dimension the canonical Hamiltonian is quite

unsuitable. Even for simple problems one has to allow the masses and the couplings to depend on the Fock space sectors [9–13]. But, in general, we need more drastic modifications. One may utilize the rich nonlocal structure of counterterms not only to remove the cutoff dependence from the low-energy observables but also to recover the lost Lorentz symmetries.

Our ultimate aim is to study the bound-state problem in QCD. However, light-front QCD is plagued with divergences arising from both small longitudinal momentum and large transverse momentum. To gain experience with the renormalization program it is useful to study a model where only one type of divergence arises. Thus, we have chosen the two-fermion bound-state problem in the $(3+1)$-dimensional light-front Yukawa model for our initial investigations.

We study the two-fermion bound-state problem in the lowest-order Tamm-Dancoff approximation retaining only two-fermion and two-fermion–one-boson states. By eliminating the three-body sector algebraically we arrive at an integral equation for the two-body state, which has both self-energy and one-boson-exchange contributions. There are divergences associated with both types of contributions. First, to discuss the renormalization aspects of the problem associated with one-boson-exchange contribution we ignore self-energy corrections and analyze the divergence associated with the ladder equation. The light-front ladder approximation has been studied previously for ϕ^3 models [14] which do not suffer from the divergence problem. A study of the pseudoscalar Yukawa model [15] has utilized form factors to regulate the divergences. Recent studies [16] on positronium emphasize the handling of the Coulomb problem in momentum space. An analysis of the asymptotic behavior of the bound-state wave function in the $(3+1)$-dimensional Yukawa model in lowest-order light-front Tamm-Dancoff approximation is carried out in Ref. [17].

In order to analyze the divergences associated with one-boson exchange and remove them via counterterms so as to renormalize the theory we use a momentum space slicing called the high-low analysis which was introduced [18] in the context of lattice theories. Here we apply it in the study of Hamiltonian renormalization problem. We refer the reader to Appendix B for an outline of this approach. A lowest-order perturbative analysis provides the so-called "box counterterm," which is nonlocal. We test the reliability of this counterterm in different helicity sectors. We also study the effect of a particular nonlocal noncanonical term in removing the divergences and renormalizing the helicity-zero sector.

After gaining some experience with the divergence problem in ladder approximation we return to the original model and study the self-energy effects. To remove the divergences we first introduce a sector-dependent mass counterterm. The remaining divergence is removed by a redefinition of the coupling constant. Here we face the well-known problem of triviality, i.e., for a fixed renormalized coupling the bare coupling becomes imaginary beyond a certain ultraviolet cutoff. This has been observed previously for the Lee model [19] and also for the meson-nucleon scattering problem in equal-time Tamm-Dancoff method [20,21]. In $3+1$ dimensions for nonzero mass of the exchanged boson the coupling has to be above a critical value for the bound states to exist. On the other hand, for a given cutoff triviality puts an upper bound on the allowed coupling constant. The interesting question is whether there exists a window where one can change cutoffs in a range considerably larger than the particle masses and compatible with couplings large enough to produce bound states. The answer is in the affirmative and we proceed to remove the cutoff dependence using boson-exchange counterterms.

The light-front Tamm-Dancoff approximation breaks rotational invariance with respect to the two transverse directions. This is visible in the spectrum which does not exhibit the degeneracy associated with the total angular momentum multiplets. As is expected the violations are very small at weak coupling and they become more visible at stronger couplings. We investigate to what extent we can recover the degeneracy by adjusting the finite parts of the counterterms, and find that the degeneracy can be removed.

The plan of this paper is as follows. In Sec. II, we derive the integral equation of the bound-state problem in the lowest-order Tamm-Dancoff approximation. Calculations in the absence of self-energy corrections are described in Sec. III and we return to self-energy corrections in Sec. IV. Section V contains our summary and conclusions. The power counting, possible structure of allowed terms in the Hamiltonian and the origin of nonlocal terms are briefly described in Appendix A. The high-low analysis is outlined in Appendix B. Finally, Appendix C contains the explicit form of the kernels in the bound-state equation before renormalization in the helicity-zero and helicity-one sectors.

II. THE FERMION NUMBER TWO SECTOR IN LOWEST-ORDER TAMM-DANCOFF APPROXIMATION

We use the following convention for light-front coordinates:

$$x^+=x^0+x^3,\quad x^-=x^0-x^3,\quad x^\perp=(x^1,x^2)\ , \tag{2.1}$$

$$a^\mu b_\mu=\tfrac{1}{2}a^+b^-+\tfrac{1}{2}a^-b^+-a^ib^i\ , \tag{2.2}$$

$$\gamma^\pm=\gamma^0\pm\gamma^3\ . \tag{2.3}$$

The projection operators

$$\Lambda^\pm=\tfrac{1}{4}\gamma^\mp\gamma^\pm \tag{2.4}$$

are used to define $\psi^+=\Lambda^+\Psi$ and $\psi^-=\Lambda^-\Psi$. The independent degrees of freedom are ψ^+, $(\psi^+)^\dagger$, and ϕ. The canonical light-front Hamiltonian for the $(3+1)$-dimensional Yukawa model is given by

$$P^-=\tfrac{1}{2}\int dx^-d^2x^\perp[2i(\psi^-)^\dagger\partial^+\psi^-+m_B^2\phi^2+\partial^\perp\phi\cdot\partial^\perp\phi]\ . \tag{2.5}$$

ψ^- can be obtained from the equation of motion and we find

$$\psi^- = \frac{1}{i\partial^+}[i\alpha^\perp\cdot\partial^\perp + \gamma^0(m_F + g\phi)]\psi^+ \ . \tag{2.6}$$

The integral operator $1/\partial^+$ is defined as

$$\frac{1}{\partial^+} f(x^-) = \tfrac{1}{4}\int dy^- \epsilon(x^- - y^-) f(y^-) \ . \tag{2.7}$$

We define

$$\psi^- = \chi^- + \eta^- \ , \tag{2.8}$$

with

$$\chi^- = \frac{1}{i\partial^+}[i\alpha^\perp\cdot\partial^\perp + \gamma^0 m_F]\psi^+ \ , \tag{2.9}$$

and

$$\eta^- = \frac{1}{i\partial^+} g\phi\psi^+ \ . \tag{2.10}$$

We define

$$\psi(x) = \psi^+(x) + \chi^-(x) \ . \tag{2.11}$$

In terms of $\psi^+(x)$, $\psi(x)$, and $\phi(x)$ we can rewrite the canonical Hamiltonian as

$$P^- = P_0^- + P_{\rm int}^- \tag{2.12}$$

with

$$P_0^- = \tfrac{1}{2}\int dx^- d^2x^\perp \left[m_B^2\phi^2 + \partial^\perp\phi\cdot\partial^\perp\phi + 2(\psi^+)^\dagger[i\alpha^\perp\cdot\partial^\perp + \gamma^0 m_F] \times \frac{1}{i\partial^+}[i\alpha^\perp\cdot\partial^\perp + \gamma^0 m_F]\psi^+ \right] \tag{2.13}$$

and

$$P_{\rm int}^- = \tfrac{1}{2}\int dx^- d^2x^\perp \left[2g\bar\psi\psi\phi + 2g^2(\psi^+)^\dagger\phi\frac{1}{i\partial^+}\phi\psi^+ \right] , \tag{2.14}$$

$$\psi(x) = \sum_\sigma \int [d^3k][b_\sigma(k)u_\sigma(k)e^{-ik\cdot x} + d_\sigma^\dagger(k)v_\sigma(k)e^{ik\cdot x}] \tag{2.15}$$

with

$$[d^3k] = \frac{dk^+ d^2k^\perp}{2(2\pi)^3 k^+} \ .$$

The destruction operators for the fermion and antifermion with momentum k and helicity σ are, respectively, $b_\sigma(k)$ and $d_\sigma(k)$. They satisfy the anticommutation relations

$$\begin{aligned} &\{b_\alpha(k), b_\beta^\dagger(k')\} = 2(2\pi)^3 k^+ \delta^3(k-k')\delta_{\alpha\beta} \ , \\ &\{d_\alpha(k), d_\beta^\dagger(k')\} = 2(2\pi)^3 k^+ \delta^3(k-k')\delta_{\alpha\beta} \ , \\ &\{b_\alpha(k), b_\beta(k')\} = 0, \quad \{d_\alpha(k), d_\beta(k')\} = 0 \ . \end{aligned} \tag{2.16}$$

The spinor

$$u_\sigma(k) = \left[\frac{1}{m_F k^+}\right]^{1/2} [m_F\Lambda^- + (k^+ + \alpha^\perp\cdot k^\perp)\Lambda^+]\chi_\sigma \ , \tag{2.17}$$

$$\chi_\uparrow = \begin{bmatrix} 1 \\ 0 \\ 0 \\ 0 \\ 0 \end{bmatrix} \sqrt{2m_F} \ ,$$

and

$$\chi_\downarrow = \begin{bmatrix} 0 \\ 1 \\ 0 \\ 0 \end{bmatrix} \sqrt{2m_F}$$

are the positive-energy solutions of the Dirac equation for a fermion at rest. The spinor $v_\sigma(k)$ is constructed from $u_\sigma(k)$ by charge conjugation. The spinors are normalized such that

$$\bar u_\sigma u_{\sigma'} = 2m_F\delta_{\sigma\sigma'}, \quad \bar v_\sigma v_{\sigma'} = -2m_F\delta_{\sigma\sigma'} \ . \tag{2.18}$$

The scalar field is given by

$$\phi(x) = \int [d^3k][a(k)e^{-ik\cdot x} + a^\dagger(k)e^{ik\cdot x}] \ , \tag{2.19}$$

$$[a(k), a^\dagger(k')] = 2(2\pi)^3 k^+ \delta^3(k-k') \ , \tag{2.20}$$

and all other commutators vanish. We consider the fermion number two sector of the theory where the two fermions belong to two different flavors. Their destruction operators are denoted by $b_\sigma(k)$ and $B_\sigma(k)$, respectively. The simplified Hamiltonian for our problem is given by

$$P^- = P_{\rm free}^- + P_{\rm int}^- \ , \tag{2.21}$$

where

$$P_{\rm free}^- = \int [d^3k]\frac{m_B^2 + k^2}{k^+} a^\dagger(k)a(k) + \sum_\sigma \int [d^3k]\frac{m_F^2 + k^2}{k^+}[b_\sigma^\dagger(k)b_\sigma(k) + B_\sigma^\dagger(k)B_\sigma(k)] \ , \tag{2.22a}$$

$$\begin{aligned} P_{\rm int}^- = g \sum_{\sigma_1,\sigma_2} &\int [d^3k_1]\int [d^3k_2]\int [d^3k_3] 2(2\pi)^3\delta^3(k_1 - k_2 - k_3) \\ &\times [b_{\sigma_1}^\dagger(k_1)b_{\sigma_2}(k_2)a(k_3)\bar u_{\sigma_1}(k_1)u_{\sigma_2}(k_2) \\ &+ b_{\sigma_2}^\dagger(k_2)b_{\sigma_1}(k_1)a^\dagger(k_3)\bar u_{\sigma_2}(k_2)u_{\sigma_1}(k_1) \\ &+ B_{\sigma_1}^\dagger(k_1)B_{\sigma_2}(k_2)a(k_3)\bar u_{\sigma_1}(k_1)u_{\sigma_2}(k_2) \\ &+ B_{\sigma_2}^\dagger(k_2)B_{\sigma_1}(k_1)a^\dagger(k_3)\bar u_{\sigma_2}(k_2)u_{\sigma_1}(k_1)] \ . \end{aligned} \tag{2.22b}$$

We have used the notation $(k^\perp)^2=k^2$. Note that we have dropped instantaneous interactions from $P^-_{\rm int}$ for simplicity.

Denote the fermion number two state that is an eigenstate of P^- with momentum P and helicity σ as $|\Psi(P,\sigma)\rangle$. The normalization is

$$\langle\Psi(P',\sigma')|\Psi(P,\sigma)\rangle=2(2\pi)^3P^+\delta^3(P-P')\delta_{\sigma\sigma'}\ . \tag{2.23}$$

In the lowest-order Tamm-Dancoff approximation,

$$\begin{aligned}|\Psi(P,\sigma)\rangle=&\sum_{\sigma_1\sigma_2}\int[d^3k_1]\int[d^3k_2]\Phi_2(P,\sigma|k_1\sigma_1,k_2\sigma_2)b^\dagger_{\sigma_1}(k_1)B^\dagger_{\sigma_2}(k_2)|0\rangle\\&+\sum_{\sigma_1\sigma_2}\int[d^3k_1]\int[d^3k_2]\int[d^3k_3]\Phi_3(P,\sigma|k_1\sigma_1,k_2\sigma_2,k_3)b^\dagger_{\sigma_1}(k_1)B^\dagger_{\sigma_2}(k_2)a^\dagger(k_3)|0\rangle\ ,\end{aligned} \tag{2.24}$$

where Φ_2 is the two-particle amplitude and Φ_3 is the three-particle amplitude and $|0\rangle$ is the vacuum state. For notational convenience we introduce the amplitudes Ψ_2 and Ψ_3:

$$\Phi_2(P,\sigma|k_1\sigma_1,k_2\sigma_2)=2(2\pi)^3P^+\delta^3(P-k_1-k_2)\sqrt{x_1x_2}\Psi_2^{\sigma_1\sigma_2}(\kappa_1^\perp x_1,\kappa_2^\perp x_2) \tag{2.25}$$

and

$$\Phi_3(P,\sigma|k_1\sigma_1,k_2\sigma_2,k_3)=2(2\pi)^3P^+\delta^3(P-k_1-k_2-k_3)\sqrt{x_1x_2x_3}\Psi_3^{\sigma_1\sigma_2}(\kappa_1^\perp x_1,\kappa_2^\perp x_2,\kappa_3^\perp x_3)\ , \tag{2.26}$$

where $x_i=k_i^+/P^+$, $\kappa_i^\perp=k_i^\perp-x_iP^\perp$. Since the wave functions are independent of the Lorentz frame we can take $P^\perp=0$ without any loss of generality. We have the constraints $\sum x_i=1$ and $\sum\kappa_i=0$. In the restricted Fock space, the normalization is

$$\begin{aligned}&\sum_{\sigma_1\sigma_2}\int dx_1dx_2\delta\left(1-\sum x_i\right)\frac{d^2\kappa_1^\perp d^2\kappa_2^\perp}{2(2\pi)^3}\delta^2\left(\sum\kappa_i^\perp\right)[\Psi_2^{\sigma_1\sigma_2}(\kappa_1^\perp x_1,\kappa_2^\perp x_2)]^2\\&\quad+\sum_{\sigma_1\sigma_2}\int dx_1dx_2dx_3\delta\left(1-\sum x_i\right)\frac{d^2\kappa_1^\perp d^2\kappa_2^\perp d^2\kappa_3^\perp}{[2(2\pi)^3]^2}\delta^2\left(\sum\kappa_i^\perp\right)[\Psi_3^{\sigma_1\sigma_2}(\kappa_1^\perp x_1,\kappa_2^\perp x_2,\kappa_3^\perp x_3)]^2=1\ .\end{aligned} \tag{2.27}$$

By projecting the equation of motion

$$[P^+P^--(P^\perp)^2]|\Psi\rangle=M^2|\Psi\rangle \tag{2.28}$$

(with $P^\perp$ set to zero) on to a set of free states we arrive at the coupled system of equations:

$$\begin{aligned}\left[M^2-\frac{m_F^2+(\kappa_1^\perp)^2}{x_1}-\frac{m_F^2+(\kappa_1^\perp)^2}{x_2}\right]\Psi_2^{\sigma_1\sigma_2}(\kappa_1^\perp,x_1)=&\frac{g}{2(2\pi)^3}\sum_{s_1}\int dy_1d^2q_1^\perp\frac{1}{\sqrt{x_1-y_1}}\Psi_3^{s_1\sigma_2}(q_1^\perp,y_1;\kappa_2^\perp,x_2)\\&\times\frac{\bar u_{\sigma_1}(\kappa_1^\perp,x_1)}{\sqrt{x_1}}\frac{u_{s_1}(q_1^\perp,y_1)}{\sqrt{y_1}}\\&+\frac{g}{2(2\pi)^3}\sum_{s_2}\int dy_2d^2q_2^\perp\frac{1}{\sqrt{x_2-y_2}}\Psi_3^{\sigma_1s_2}(\kappa_1^\perp,x_1;q_2^\perp,y_2)\\&\times\frac{\bar u_{\sigma_2}(\kappa_2^\perp,x_2)}{\sqrt{x_2}}\frac{u_{s_2}(q_2^\perp,y_2)}{\sqrt{y_2}}+\text{counterterms}\end{aligned} \tag{2.29}$$

and

$$\begin{aligned}&\left[M^2-\frac{m_F^2+(\kappa_1^\perp)^2}{x_1}-\frac{m_F^2+(\kappa_2^\perp)^2}{x_2}-\frac{m_B^2+(\kappa_1^\perp+\kappa_2^\perp)^2}{x_3}\right]\Psi_3^{\sigma_1\sigma_2}(\kappa_1^\perp,x_1;\kappa_2^\perp,x_2)\\&\quad=g\sum_{s_1}\frac{1}{\sqrt{x_3}}\Psi_2^{s_1\sigma_2}(-\kappa_2^\perp,x_1+x_3)\frac{\bar u_{\sigma_1}(\kappa_1^\perp,x_1)}{\sqrt{x_1}}\frac{u_{s_1}(-\kappa_2^\perp,x_1+x_3)}{\sqrt{x_1+x_3}}\\&\quad+g\sum_{s_2}\frac{1}{\sqrt{x_3}}\Psi_2^{\sigma_1s_2}(\kappa_1^\perp,x_1)\frac{\bar u_{\sigma_2}(\kappa_2^\perp,x_2)}{\sqrt{x_2}}\frac{u_{s_2}(-\kappa_1^\perp,x_2+x_3)}{\sqrt{x_2+x_3}}+\text{counterterms}\ .\end{aligned} \tag{2.30}$$

After eliminating Ψ_3 one ends up with the following equation involving Ψ_2 and the eigenvalue M^2:

$$M^2\Psi_2^{\sigma_1\sigma_2}(\kappa^\perp,x)=(M_0^2+T_{\rm SE})\Psi_2^{\sigma_1\sigma_2}(\kappa^\perp,x)+\frac{\alpha}{4\pi^2}\sum_{s_1,s_2}\int d^2q^\perp dy\, K(\kappa^\perp,x;q^\perp,y;M^2)^{\sigma_1\sigma_2,s_1s_2}\Psi^{s_1s_2}(q^\perp,y)+\text{counterterms}\ , \tag{2.31}$$

where

$$M_0^2=\frac{m_F^2+k^2}{x(1-x)} \tag{2.32}$$

and

$$\alpha=\frac{g^2}{4\pi}\ .$$

$T_{\rm SE}$ is the self-energy term that is generated when Ψ_3 is eliminated and the boson is reabsorbed by the fermion that emitted it:

$$T_{\rm SE}=-\frac{\alpha}{4\pi^2}\int d^2q^\perp dy\left\{\frac{1}{x}\left[\frac{1}{y}+\frac{[M^2-(m_F^2+k^2)/x(1-x)]x(1-y)+[4m_F^2-m_B^2]}{\text{denominator}}\right]+[x\to(1-x)]\right\}, \tag{2.33}$$

$$\text{denominator}=q^2+ym_B^2+\frac{y(1-y)}{1-x}k^2+\frac{(1-y)(1-x+xy)}{1-x}m_F^2-y(1-y)xM^2\ , \tag{2.34}$$

and K is the boson-exchange kernel,

$$K(\kappa^\perp,x;q^\perp,y;M^2)^{\sigma_1\sigma_2,s_1s_2}=\frac{\dfrac{\bar u(\kappa^\perp,x;\sigma_1)u(q^\perp,y;s_1)}{\sqrt{xy}}\dfrac{\bar u(-\kappa^\perp,1-x;\sigma_2)u(-q^\perp,1-y;s_2)}{\sqrt{(1-x)(1-y)}}}{a+2(\kappa^\perp\cdot q^\perp)}\ , \tag{2.35}$$

$$a=|x-y|\left[M^2-\frac{1}{2}\left[\frac{m_F^2+k^2}{x(1-x)}+\frac{m_F^2+q^2}{y(1-y)}\right]\right]-m_B^2+2m_F^2-\frac{m_F^2+k^2}{2}\left[\frac{y}{x}+\frac{1-y}{1-x}\right]-\frac{m_F^2+q^2}{2}\left[\frac{x}{y}+\frac{1-x}{1-y}\right]. \tag{2.36}$$

Equation (2.31) is schematically shown in Fig. 1. The *counterterms* in Eq. (2.31) are necessary to remove divergences both in the "self-energy" term $T_{\rm SE}$ and in the "boson-exchange term" involving the kernel $K(\kappa^\perp,x;q^\perp,y;M^2)$. $T_{\rm SE}$ has an ultraviolet quadratically diverging term (which also has an "infrared" logarithm at $y\to0$) and a subleading ultraviolet logarithmically diverging contribution. In the lowest-order Tamm-Dancoff approximation these can be removed via the analogue of mass and wave-function renormalization. This will be described in detail in Sec. IV. We will see that wave-function renormalization can be absorbed as a "partial" coupling constant renormalization. We say "partial" here because the Tamm-Dancoff truncation does not allow for vertex corrections and the coupling "runs" solely due to Z_2. This, however, does not change the sign of the β function and one sees that even in lowest-order Tamm-Dancoff the "triviality problem" of nonasymptotically free theories is revealed. Restrictions coming from triviality will be explained and quantified again in Sec. IV. Suffice it here to mention that due to triviality one should not attempt to take the ultraviolet cutoff to ∞ if one wants the renormalized coupling to be nonvanishing, and hence to have interesting physics such as bound states. On the other hand, even granting the presence of a finite cutoff, one still requires that the low-energy physics be insensitive to where exactly this cutoff is placed.

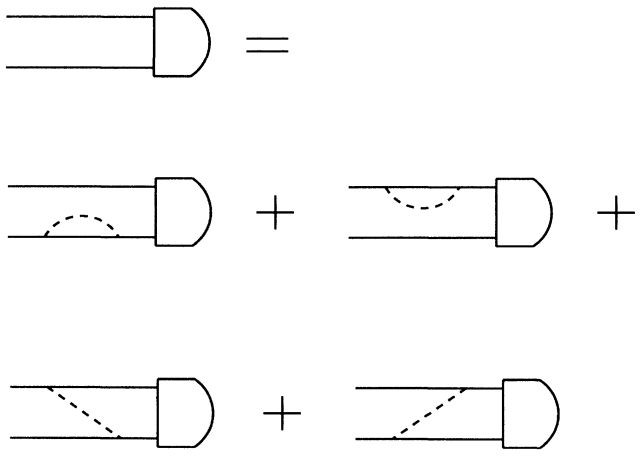

FIG. 1. The schematic representation of the light-front Tamm-Dancoff equation. The second line represents self-energy contributions and the third line represents boson-exchange contributions.

The other possible source of divergences lies in the next to last term in Eq. (2.31). The kernel K has terms that go to a function of only x and y as $|q^\perp|\to\infty$. So unless Ψ_2 vanishes faster than $|q^\perp|^{-2}$ the integral over $d^2q^\perp$ will diverge. We find in our calculations that many spin components of Ψ_2 fall off only as $|q^\perp|^{-2}$ for large $|q^\perp|$ and

not faster. So we are forced to include counterterms to remove this divergence. We will call these counterterms Boson-exchange counterterms as opposed to the self-energy counterterms of the previous paragraph. The boson-exchange counterterms represent a new type of counterterm that does not have an analogue in equal-time perturbation theory. In order to investigate these new counterterms in isolation, we consider a simplified model in the next section in which T_{SE} is dropped from Eq. (2.31) and all self-energy corrections including triviality considerations are ignored. After experimenting with several ways to handle boson-exchange counterterms, we then go back, in Sec. IV, to the full problem, Eq. (2.31).

Our set of three-dimensional coupled TD integral equations, Eq. (2.31), can be reduced to two-dimensional equation by taking advantage of helicity conservation. We first expand

$$\Psi_2^{\sigma_1\sigma_2}(\kappa^\perp,x)=\sum_m \frac{e^{im\phi}}{\sqrt{2\pi}}\Phi^{\sigma_1\sigma_2}(k,x;m) \tag{2.37}$$

where $k=|\kappa^\perp|$. In the $\{\Phi^{\sigma_1\sigma_2}(k,x;m)\}$ basis the kernel in Eq. (2.31) becomes

$$V(k,x,m;q,y,m';M^2)^{\sigma_1\sigma_2,s_1s_2} = \int \frac{d\phi\, d\phi'}{2\pi} e^{-im\phi} e^{im'\phi'} K(k,\phi,x;q,\phi',y;M^2)^{\sigma_1\sigma_2,s_1s_2} . \tag{2.38}$$

Because of helicity conservation, the kernel V will be such that for given J_z value only four amplitudes $\Phi^{\sigma_1\sigma_2}(k,x;m)=\Phi^{\uparrow\uparrow}(k,x;J_z-1)$, $\Phi^{\uparrow\downarrow}(k,x;J_z)$, $\Phi^{\downarrow\uparrow}(k,x;J_z)$, and $\Phi^{\downarrow\downarrow}(k,x;J_z+1)$ contribute. So one has at most a system of four coupled integral equations to solve. The ϕ integrals in Eq. (3.28) can be done analytically. One finds that the divergence structure for the remaining q integral depends on which J_z sector one is dealing with. Only in the $J_z=0$ and $J_z=\pm1$ sectors does one need a boson-exchange counterterm.

In the $J_z=0$ sector one can further reduce the number of equations that are coupled so that one only needs to deal with systems of two coupled equations. Using the notation

$$\Phi^{1\pm}(k,x)=\frac{1}{\sqrt{2}}[\Phi^{\uparrow\uparrow}(k,x;-1)\pm\Phi^{\downarrow\downarrow}(k,x;1)] ,$$
$$\Phi^{2\pm}(k,x)=\frac{1}{\sqrt{2}}[\Phi^{\uparrow\downarrow}(k,x;0)\pm\Phi^{\downarrow\uparrow}(k,x;0)] , \tag{2.39}$$

one finds that Φ^{1+},Φ^{2-} and Φ^{1-},Φ^{2+} mix, respectively, with each other. We will refer to these two sets in the future as the $(1+,2-)$ and $(1-,2+)$ sectors. We will see that preponderance of the wave function will be in either 2^- which has the singlet spin configuration or 2^+ which has the triplet spin configuration.

III. CALCULATIONS IN THE ABSENCE OF SELF-ENERGY CORRECTIONS

In this section we discuss renormalization of Eq. (2.31) and the bound-state spectrum of the fermion number two sector ignoring the effects of self-energy corrections, i.e., after dropping the T_{SE} term in Eq. (2.31). We first investigate what happens if one just introduces an ultraviolet cutoff Λ to regularize $|\kappa^\perp|$ and $|q^\perp|$ and do not include any counterterms at all. This will demonstrate how severe the divergence structure is. We will see that boson-exchange counterterms are required in the $J_z=0$ and $J_z=\pm1$ helicity sectors.

A. Results without counterterms

1. $J_z=0$

The relevant equations in this sector are

$$(M^2-M_0^2)\Phi^{1-}(k,x)=\frac{\alpha}{4\pi^2}\int q\,dq\,dy\{V(k,x;q,y;M^2)^{1-,1-}\Phi^{1-}(q,y)+V(k,x;q,y;M^2)^{1-,2+}\Phi^{2+}(q,y)\} , \tag{3.1a}$$

$$(M^2-M_0^2)\Phi^{2+}(k,x)=\frac{\alpha}{4\pi^2}\int q\,dq\,dy\{V(k,x;q,y;M^2)^{2+,1-}\Phi^{1-}(q,y)+V(k,x;q,y;M^2)^{2+,2+}\Phi^{2+}(q,y)\} , \tag{3.1b}$$

and there is another set of coupled equations with $\Phi^{1-}(\Phi^{2+})$ replaced by $\Phi^{1+}(\Phi^{2-})$. The explicit form of the kernels V are given in Appendix C. One finds that $V^{2-,2-}$ and $V^{2+,2+}$ both approach a function of x and y, independent of k or q for large q relative to k:

$$\lim_{q\gg k} V(k,x;q,y;M^2)^{2\pm,2\pm}=\mp f(x,y) = \mp\frac{4\pi}{x(1-y)+y(1-x)+|x-y|} . \tag{3.2}$$

We will see in a moment that $\Phi^{2\pm}$ fall off as q^{-2} for large q. So this information combined with Eq. (3.2) tells us that one can expect the q integral in Eq. (3.1b) to diverge logarithmically with the cutoff Λ. This diverging contribution comes in with opposite signs in the $(1-,2+)$ and $(1+,2-)$ sectors. In the former sector one has an "attractive diverging potential" whereas in the latter sector the diverging contribution is "repulsive." Hence cutoff effects are likely to be more severe in the $(1-,2+)$ sector. These expectations are born out by our calculations.

We have solved Eq. (3.1) using Gauss-Legendre quadrature to evaluate the q and y integrals. By restricting the external variables, k and x, also to just the quadrature points one ends up with a finite matrix problem. Note that the "eigenvalue," M^2, appears on both the left- and right-hand side (RHS) of Eq. (3.1). We dealt with this by first inserting a guess for $M^2 \rightarrow M^2_{\text{input}}$ on the RHS and solving the resulting matrix eigenvalue problem to obtain an output M^2_{output} which then became the M^2_{input} for the next iteration. This procedure was iterated until $M^2_{\text{output}} = M^2_{\text{input}}$ to one part in 10^4. Usually four or five iterations sufficed to achieve convergence. We use N_1 quadrature points for the q (and k) variable and N_2 points for y (and x). More precisely, we first changed variables from (k,x) to $z = 2[k(\Lambda + m_F)/(k + m_F)\Lambda] - 1$ and $\bar{x} = 2x - 1$ and picked Gauss-Legendre quadrature points for these new variables. To solve the matrix eigenvalue problem we have used the EISPACK [22] routines. Most of our data come from $(N_1, N_2) = (8, 32)$. We have checked that results for M^2 are stable with respect to changes in N_1 and N_2 to one part in 10^3. For our parameters we chose $m_B = 0.25$, 0.5 (all masses are measured in units of the fermion mass m_F), and $\alpha = 0.395$, 1.184, 1.579, 1.974. In Fig. 2, we show results for $m_B = 0.25$ and $\alpha = 1.184$. For these parameters we find one bound state each in the $(1-,2+)$ and $(1+,2-)$ sectors and plot the bound state M^2 as a function of the cutoff Λ (note that with our convention of measuring everything in units of the fermion mass, the threshold is at $M^2 = 4$). From Fig. 2 one sees that there is sensitivity to the cutoff and that it is worse for the $(1-,2+)$ states. Clearly some counterterm must be included in the calculations to eliminate cutoff dependence.

In Figs. 3(a) and 3(b) we show plots of $k^2\Phi^{1\pm}(k,x)$ and $k^2\Phi^{2\pm}(k,x)$ versus k at fixed x for $m_B = 0.25$, $\alpha = 1.184$, and $\Lambda = 50$. One sees $k^2\Phi$ approaching nonzero constants for large k, indicating that Φ is behaving as k^{-2}.

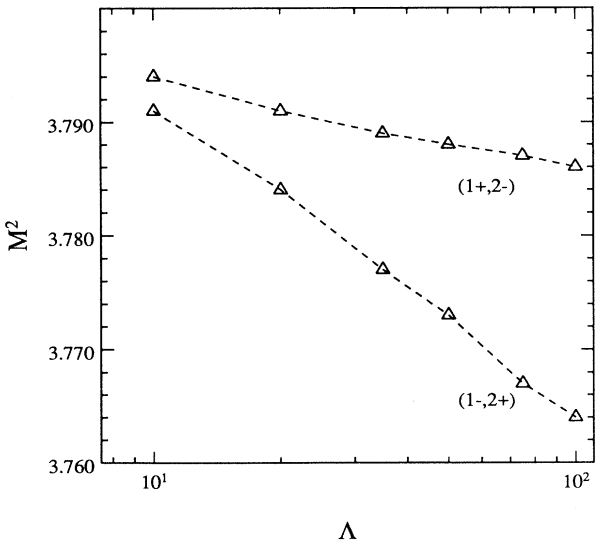

FIG. 2. The bound-state mass M^2 vs the cutoff Λ in the helicity-zero sector for $m_B = 0.25$ and $\alpha = 1.184$.

In Figs. 4(a)–4(d) we present $|\Phi|$ versus k and x for the same parameters. Note that the wave functions are plotted on an arbitrary scale to show the shape of the various wave functions. The large components are in Figs. 4(b) and 4(d). Also note that the wave functions in Figs. 4(a) and 4(c) peak away from $k = 0$ indicating an $l \neq 0$ component.

Useful information can be obtained by calculating the relative strengths of the different spin contributions to the eigenfunctions. We evaluate

$$\text{Norm}^{i\pm} = \int k\, dk\, dx\, |\Phi^{i\pm}(k,x)|^2 \tag{3.3a}$$

normalized such that

$$\text{Norm}^{1-} + \text{Norm}^{2+} = \text{Norm}^{1+} + \text{Norm}^{2-} = 1\ . \tag{3.3b}$$

The results are presented in Table I(a) for weak coupling $\alpha = 0.395$, $m_B = 0.1$ and Table I(b) for strong coupling

TABLE I. Relative norm of two-particle states. (a) $m_B = 0.1$, $\alpha = 0.395$. (b) $m_B = 0.5$, $\alpha = 1.974$. (c) $m_B = 0.1$, $\alpha = 0.395$. (d) $m_B = 0.5$, $\alpha = 1.974$.

Helicity	M^2		State	Norm
		(a)		
		$1-$	$\frac{\uparrow\uparrow - \downarrow\downarrow}{\sqrt{2}}$	0.0000
0	3.972			
		$2+$	$\frac{\uparrow\downarrow + \downarrow\uparrow}{\sqrt{2}}$	1.0000
		$1+$	$\frac{\uparrow\uparrow + \downarrow\downarrow}{\sqrt{2}}$	0.0122
0	3.972			
		$2-$	$\frac{\uparrow\downarrow - \uparrow\downarrow}{\sqrt{2}}$	0.9878
		(b)		
		$1-$	$\frac{(\uparrow\uparrow - \downarrow\downarrow)}{\sqrt{2}}$	0.0018
0	3.494			
		$2+$	$\frac{\uparrow\downarrow + \uparrow\downarrow}{\sqrt{2}}$	0.9982
		$1+$	$\frac{\uparrow\uparrow + \downarrow\downarrow}{\sqrt{2}}$	0.1102
0	3.579			
		$2-$	$\frac{\uparrow\downarrow - \uparrow\downarrow}{\sqrt{2}}$	0.8898
		(c)		
			$\uparrow\uparrow$	0.9938
			$\uparrow\downarrow$	0.0031
1	3.972			
			$\downarrow\uparrow$	0.0031
			$\downarrow\downarrow$	0.0000
		(d)		
			$\uparrow\uparrow$	0.9444
			$\uparrow\downarrow$	0.0261
1	3.575			
			$\downarrow\uparrow$	0.0261
			$\downarrow\downarrow$	0.0034

$\alpha=1.184$, $m_B=0.25$. One sees that in both the $(1-,2+)$ and $(1+,2-)$ sectors the $S_z=0$ spin configuration, $(\uparrow\downarrow\pm\downarrow\uparrow)$, dominates over $\uparrow\uparrow$ or $\downarrow\downarrow$. Recall that neither S_z nor L_z are independently conserved and only $J_z=S_z+L_z$ is a good quantum number. The fact that the lowest states in the $J_z=0$ sector have predominantly $S_z=0$ spin content tells us that $L_z>0$ contributions are small. Table I shows, however, that contributions from higher L_z increases gradually with the coupling α. The predominance of $L_z=0$ persists also when we later include counterterms into our calculations.

2. $J_z=1$

In this sector one must solve a system of four coupled integral equations. The amplitudes $\Phi^{\uparrow\uparrow}(k,x;m=0)$, $\Phi^{\uparrow\downarrow}(k,x;1)$, $\Phi^{\downarrow\uparrow}(k,x;1)$, and $\Phi^{\downarrow\downarrow}(k,x;2)$ are coupled to each other. The relevant kernels $V(k,x;q,y;M^2)^{\sigma_1\sigma_2,s_1s_2}$ are listed in Appendix C. One finds that the kernel $V^{\uparrow\uparrow,\downarrow\downarrow}$ approaches the same limit $-f(x,y)$ as in Eq. (3.2) when q becomes large relative to k. All other kernels fall off faster with q. Using the same methods as described above for the $J_z=0$ sector, we have calculated M^2. For

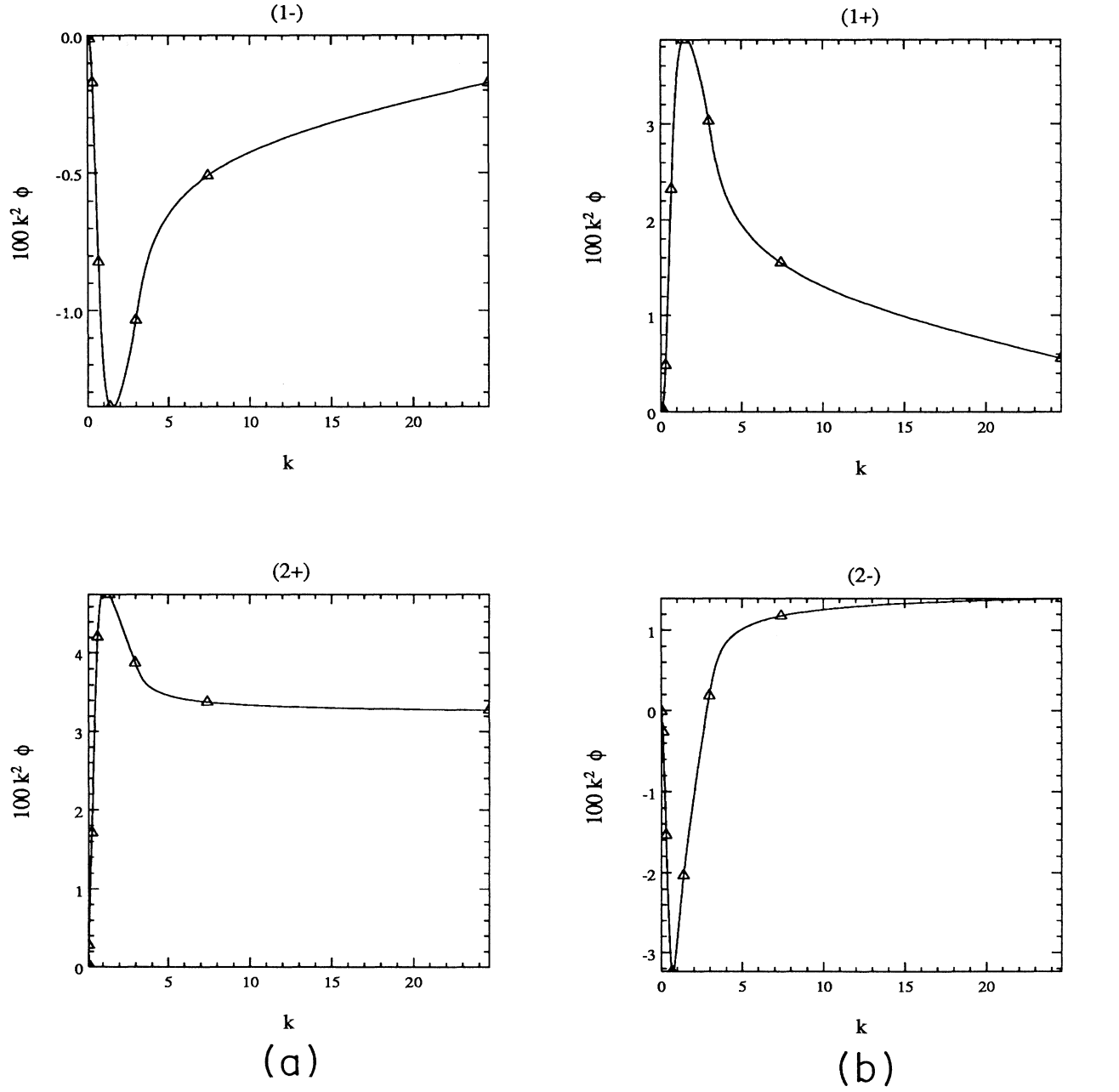

FIG. 3. (a) $k^2\Phi$ vs k at fixed x for the $(1-)$ and $(2+)$ states for $m_B=0.25$, $\alpha=1.184$, and $\Lambda=50$. (b) Same as in (a) but for the $(1+)$ and $(2-)$ states.

the same set of parameters as in Fig. 2 ($\alpha=1.184$ and $m_B=0.25$) one finds only one bound state. In Fig. 5, we plot M^2 versus the cutoff Λ. In the $J_z=1$ sector, due to the behavior of V it appears counterterms are necessary to eliminate cutoff dependence. The spin content and norm of the single bound state that occurs in $J_z=1$ sector in a weak coupling is given in Table I(c) and the strong coupling in Table I(d). One sees that here the dominant contribution comes from $\Phi^{\uparrow\uparrow}(k,x;m=0)$, showing once again, as in the $J_z=0$ sector, that $L_z>0$ contributions to the lowest bound state are small.

Note that for strong coupling [Tables I(b) and I(d)] the states are no longer degenerate. There is a ground state with mass $M^2=3.494$. If one were to associate the remaining states with $J=1$ and $J_z=0$ and 1 we would expect them to be degenerate, they are not. We will return to this point after including counterterms.

3. $J_z>1$

An analysis of the bound-state equation (2.31) indicates that the $J_z>1$ helicity sectors are free of boson-exchange divergences. While there were no bound states for the parameter used above if we increase α significantly we can generate a bound state in $J_z=2$. In Fig. 6 we plot M^2 versus the cutoff Λ for the parameters $\alpha=3.948$ and $m_B=0.25$ for $J_z=2$. As expected there is no significant cutoff dependence.

B. Counterterms

We now turn to renormalization of the bound-state equations. The purpose of including counterterms is twofold: (1) to eliminate cutoff (Λ) dependence and (2) to allow for sufficient flexibility in the finite parts of the counterterm to be able to renormalize to some experimental input. In Appendix B, we show in simple models that it is possible to add counterterms that completely remove all the cutoff dependence from both the wave functions and the bound-state spectrum. In one-dimensional models the finite part of the counterterm contains an arbitrary dimensionful scale μ and an associated arbitrary constant. In two-dimensional models the arbitrary con-

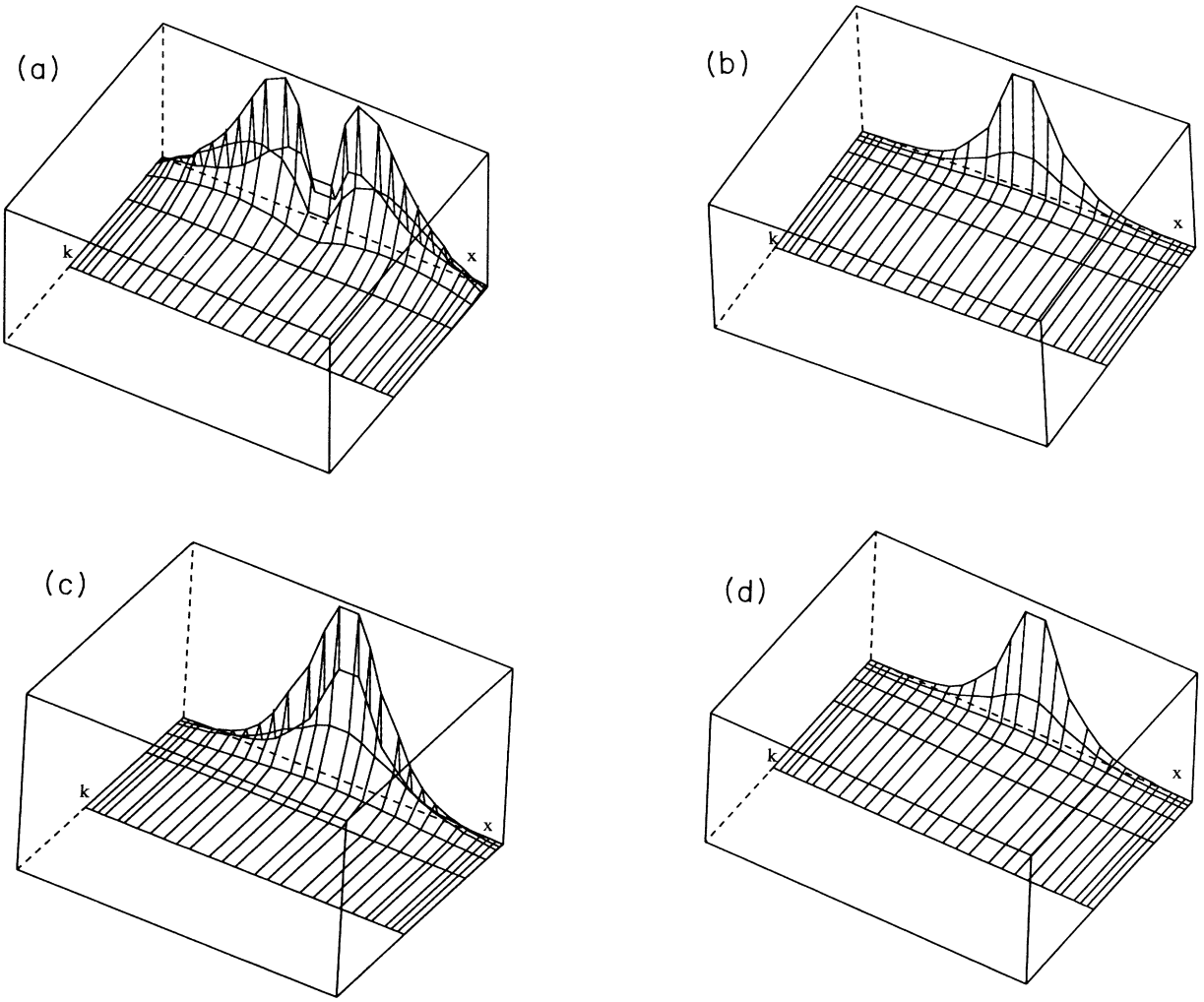

FIG. 4. (a) $|\Phi|$ vs k and x for the $(1-)$ state for $m_B=0.25$, $\alpha=1.184$, and $\Lambda=50$. Arbitrary scale. (b) Same as in (a) but for the $(2+)$ state. (c) Same as in (a) but for the $(1+)$ state. (d) Same as in (a) but for the $(2-)$ state.

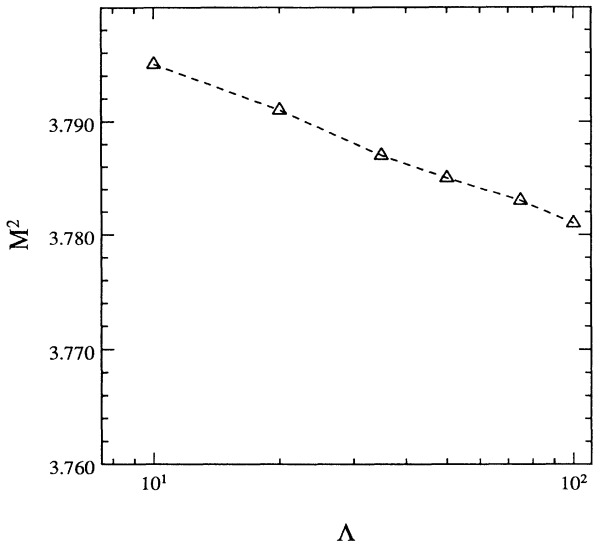

FIG. 5. The bound-state mass M^2 vs the cutoff Λ in the helicity-one sector for $m_B=0.25$ and $\alpha=1.184$.

stant becomes an arbitrary function. It is convenient to subdivide the study of these counterterms into two categories. One we will call the asymptotic counterterms, and the other we will call the perturbative counterterms.

1. Perturbative counterterm

Studies of the simple models discussed in Appendix B and the general power counting arguments of Appendix A show that equations such as Eq. (3.1) should be supplemented by a counterterm of the form

$$G(\Lambda)\int q\,dq\,dy\,F(x,y)\phi(q,y)\ . \tag{3.4}$$

For the Yukawa model we have not been able to solve for

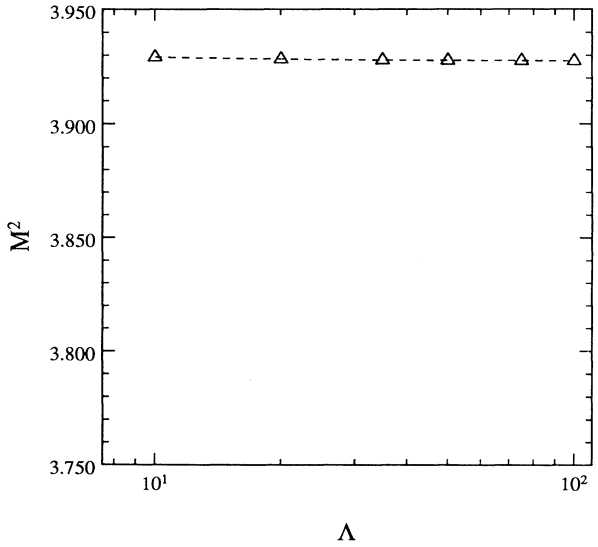

FIG. 6. The bound-state mass M^2 vs the cutoff Λ in the helicity-two sector for $m_B=0.25$ and $\alpha=3.948$.

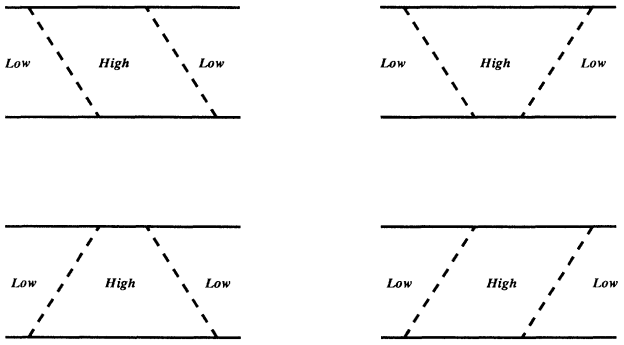

FIG. 7. Fourth-order light-front time-ordered diagrams for the two-body interaction which give rise to the box counterterm.

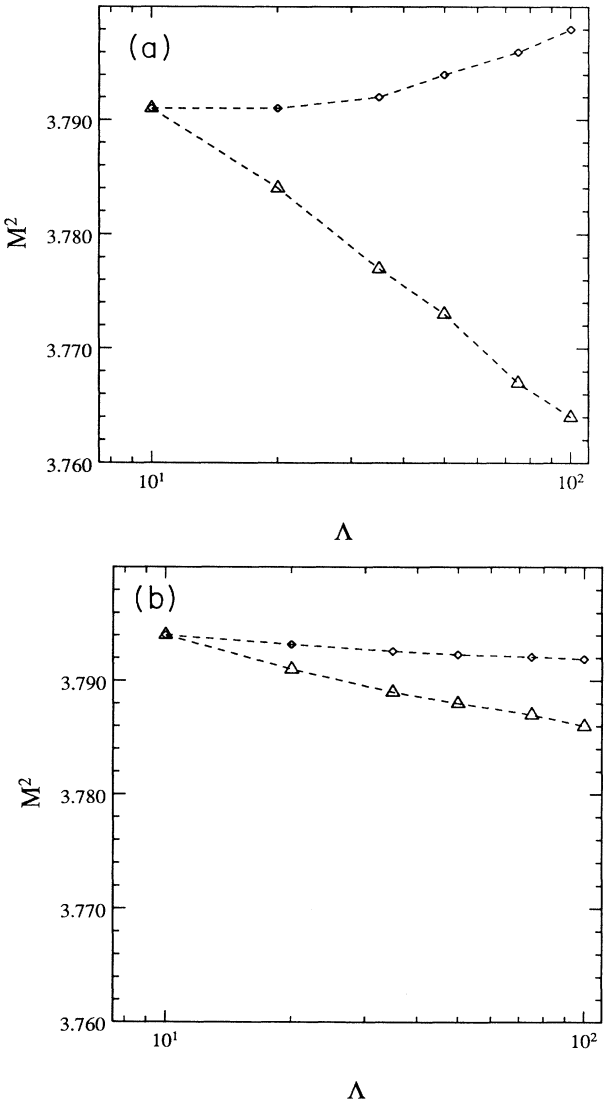

FIG. 8. (a) The bound-state mass M^2 vs the cutoff Λ in the helicity-zero sector for the state $(1-,2+)$ for $m_B=0.25$ and $\alpha=1.184$. No counterterm, dashed (triangle); one box counterterm ($C=2.3026$), dot-dashed (diamond). (b) Same as in (a) but for the state $(1+,2-)$.

$G(\Lambda)F(x,y)$ exactly. One can, however, estimate $G(\Lambda)F(x,y)$ perturbatively. The lowest-order (order α^2) perturbative counterterms correspond to graphs shown in Fig. 7. We call these "box counterterms." Applying Eq. (B30) of Appendix B to the Yukawa model, one finds that Eq. (3.1) should be modified according to

$$V(k,x;q,y;M^2)^{2+,2+} \rightarrow V(k,x;q,y;M^2)^{2+,2+} - V^{\mathrm{BCT}}(x,y) , \quad (3.5)$$

where

$$V^{\mathrm{BCT}}(x,y) = -(\alpha)^2[C+\ln(\Lambda)]\left\{\Theta(x-y)\left[\frac{x-y}{x(1-y)} - \frac{1}{x} - \frac{\ln(1-y)}{xy} - \frac{\ln x}{(1-x)(1-y)} - \frac{1}{1-y}\right] + \Theta(y-x)[x\leftrightarrow y]\right\} . \quad (3.6)$$

Similarly,

$$V(k,x;q,y;M^2)^{2-,2-} \rightarrow V(k,x;q,y;M^2)^{2-,2-} - V^{\mathrm{BCT}}(x,y) \quad (3.7)$$

and, in the $J_z=1$ sector

$$V(k,x;q,y;M^2)^{\uparrow\uparrow,\uparrow\uparrow} \rightarrow V(k,x;q,y;M^2)^{\uparrow\uparrow,\uparrow\uparrow} - V^{\mathrm{BCT}}(x,y) . \quad (3.8)$$

C in Eq. (3.6) is an arbitrary adjustable constant. We have redone our bound-state mass calculations with the modifications (3.5), (3.7), and (3.8). The results are presented in Figs. 8 and 9 for $m_B=0.25$, $\alpha=1.184$, and $C=2.3026$. In Fig. 8, we show the results with and without the box counterterm for $J_z=0$. In Fig. 9, we show the same effect for $J_z=1$. Results for other C values are summarized in Table II. One sees that the cutoff independence is improved. So one has an (almost) finite calculation involving arbitrary parameters, namely, a different C for each sector. One could consider adjusting the parameters to fix (1) the absolute scale of the bound-state energies, (2) the splitting between the two states in the $J_z=0$ sector, and (3) the $J_z=1$ bound state relative to the $J_z=0$ states. The last adjustment, i.e., the tuning of the $J_z=1$ state could be exploited to try to force the spectrum into j multiplets. That means, if we interpret Table I to imply that $l>0$ orbital momentum contributions are small, that the $J_z=1$ state should be made degenerate with the $J_z=0$ $(1-,2+)$ state. The $J_z=1$ state (and a similar $J_z=-1$ state) together with the $(1-,2+)$ state will then form a $j=1$ triplet level. The remaining $(1+,2-)$ state in the $J_z=0$ sector could be interpreted as a $j=0$ singlet level. Table II shows us that for the m_B and α values chosen, all eigenvalues do not depend strongly on either C or the state. Adjusting the C's allows us to move eigenvalues around only in a limited way. It is possible, however, to make the $J_z=1$ state degenerate with either of the two $J_z=0$ states. The splitting among the two $J_z=0$ states remain small. Not surprisingly one cannot take too large C's without generating strong cutoff dependence.

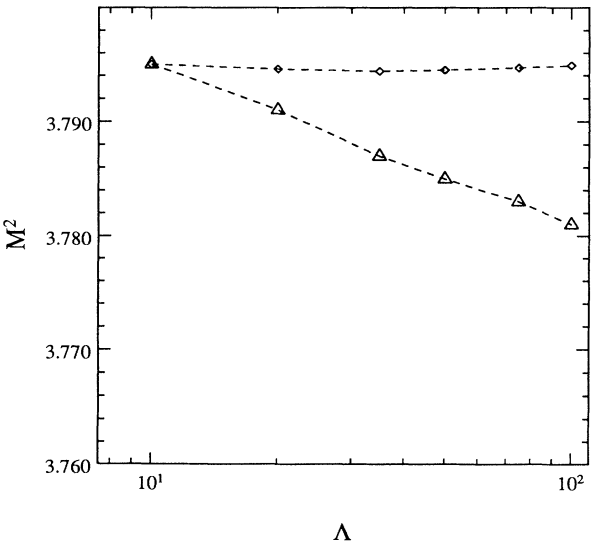

FIG. 9. The bound-state mass M^2 vs the cutoff Λ in the helicity-one sector for $m_B=0.25$ and $\alpha=1.184$. No counterterm, dashed (triangle); one box counterterm ($C=2.3026$), dot-dashed (diamond).

We emphasize that the box counterterm is only an approximation to the full counterterm required to renormalize the bound-state equations. It introduces the constants C and we have tried to use them to impose rotational symmetry on the small number of bound states at hand. In the future one will have to seriously explore ways to adjust arbitrary functions rather than constants. In the box diagram we have picked a particular function [Eq. (3.6)], dictated by perturbation theory, and adjusted just the coefficient multiplying it. One way to improve on the present calculations may be to expand the "arbitrary function" in terms of a complete set and systematically increase the number of terms kept in the expansion. The expansion coefficients will be the analogues of the current C's.

2. *Asymptotic counterterm*

We have also explored the possibility of eliminating divergences nonperturbatively by subtracting the large transverse momentum limit of the kernel. This type of counterterm we call the asymptotic counterterm. In the Yukawa model we have been able to employ such counterterms only in the $J_z=0$ sector. Instead of Eqs. (3.5) and (3.7) one then has

$$V(k,x;q,y;M^2)^{2+,2+} \rightarrow V(k,x;q,y;M^2)^{2+,2+} + V^{\mathrm{ACT}}(x,y)\ , \quad (3.9)$$

$$V(k,x;q,y;M^2)^{2-,2-} \rightarrow V(k,x;q,y;M^2)^{2-,2-} - V^{\mathrm{ACT}}(x,y) \quad (3.10)$$

with

$$V^{\mathrm{ACT}}(x,y) = f(x,y) \quad (3.11)$$

of Eq. (3.2). One can show that this extra term would arise if one added to the canonical light-front Hamiltonian of Eq. (2.5) another term:

$$P^-_{\mathrm{ACT}} = \frac{g^2}{4}\int d^2x^\perp dx^- dy^- \left\{ \left[\left[\frac{1}{-i\partial_x^+}\bar{\psi}_{u^1} \right] \gamma^+\gamma_\perp \psi_{u^1} \right]_{(x^-,\mathbf{x}_\perp)} \frac{2\pi i}{x^- - y^- - i\epsilon} \left[\bar{\psi}_{u^2}\gamma^+\gamma_\perp \left[\frac{1}{i\partial_y^+}\psi_{u^2} \right] \right]_{(y^-,\mathbf{x}_\perp)} + \mathrm{H.c.} \right\}, \quad (3.12)$$

where ψ_{u^i} stands for the $u(k)$ part of the fermion field ψ in Eq. (2.15) for fermion type i. The additional interaction (3.12), although not part of the canonical Hamiltonian, is allowed by power counting rules of light-front quantized field theory. But we note that g in front of this term has to precisely match the g in the canonical Hamiltonian. The power of g is the same as in the effective Hamiltonian in the two-body sector. Hence a term such as Eq. (3.12) cannot be created perturbatively. Such a term would not be acceptable in a renormalization program based on perturbation theory to all orders in the coupling, where it is assumed that arbitrary constants and functions are small.

In Figs. 10(a) and 10(b) we show the results for the lowest bound states in the $J_z=0$ $(1-,2+)$ and $(1+,2-)$ sectors, both with (squares) and without (triangles) the counterterm V^{ACT}. One sees that with the asymptotic counterterm cutoff dependence has been eliminated for

TABLE II. Flexibility with box counterterm. (a) $(1-,2+)$ state. (b) $(1+,2-)$ state. (c) Helicity-one state.

Λ	C	M^2	Λ	C	M^2
	(a)				
				−2.3026	
10		3.810	50		3.792
20		3.812	75		3.792
35		3.814	100		3.792
	0.0				
50		3.816	10		3.786
75		3.818	20		3.786
100		3.820	35		3.786
				−4.4998	
10		3.791	50		3.786
20		3.791	75		3.786
35		3.792	100		3.786
	−2.3026				
50		3.794		(c)	
75		3.796	10		3.807
100		3.798	20		3.806
			35		3.806
10		3.769		0.0	
20		3.765	50		3.806
35		3.764	75		3.806
	−4.4998		100		3.806
50		3.764			
75		3.764	10		3.795
100		3.766	20		3.795
			35		3.794
	(b)			−2.3026	
10		3.802	50		3.794
20		3.800	75		3.795
35		3.799	100		3.795
	0.0				
50		3.798	10		3.782
75		3.797	20		3.781
100		3.797	35		3.781
				−4.4998	
10		3.794	50		3.781
20		3.793	75		3.782
35		3.793	100		3.782

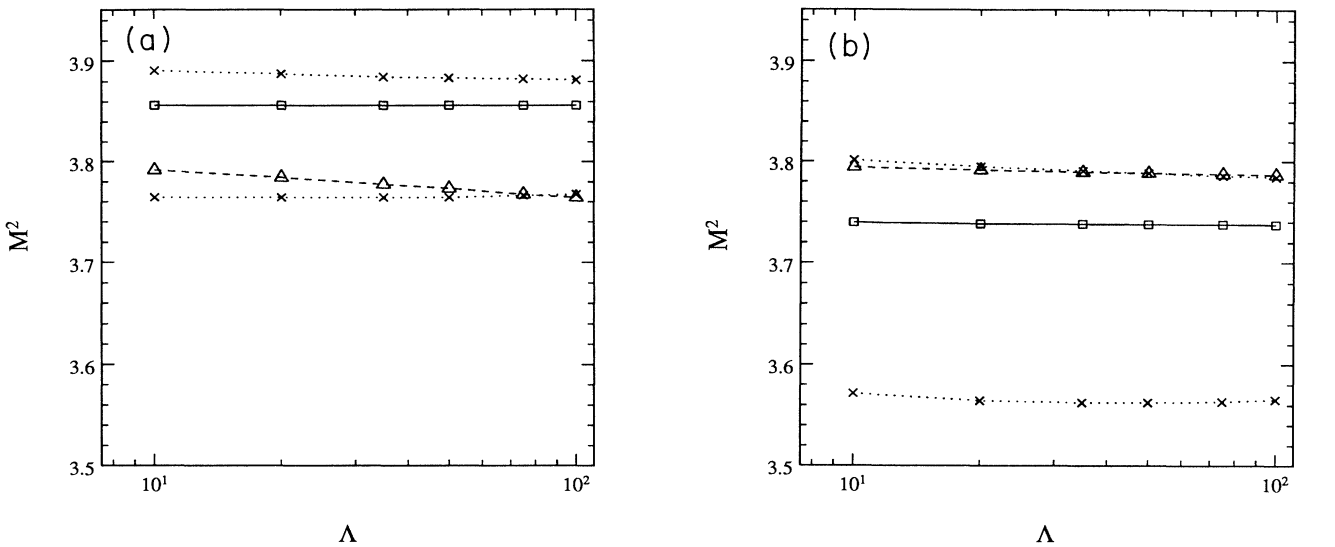

FIG. 10. (a) The bound-state mass M^2 vs the cutoff Λ in the helicity-zero sector for the channel $(1-,2+)$ for $m_B=0.25$ and $\alpha=1.184$. No counterterm, dashed (triangle); asymptotic counterterm, solid (square); asymptotic plus constant, dotted (cross). The two dotted lines correspond to the two different choices of the constant counterterm which differ only by a sign. (b) Same as in (a) but for the channel $(1+,2-)$.

the $(1-,2+)$ states and improved for the $(1+,2-)$ states. We also find that this counterterm modifies the large-k behavior of the amplitudes $\Phi(k,x)$ making them fall off faster than before.

The asymptotic counterterm, as it stands, does not include any arbitrary constants that can be tuned to renormalize the theory to some experimental input. This differs from the case with the box counterterm where such a constant appeared. One may, however, add to $V^{\rm ACT}$ an adjustable piece, which, in general, involves an arbitrary function of longitudinal momenta. In the present investigation we have added a simple term to $V^{\rm ACT}$, motivated by Eq. (B22) in Appendix B. The coefficient of this term then introduces some flexibility in adjusting energy levels. In (3.9) and (3.10) we replace

$$V^{\rm ACT}\to V^{\rm ACT}-G_\Lambda\ , \tag{3.13}$$

where we take, for G_Λ,

$$G_\Lambda=\frac{G_\mu}{1+(G_\mu/6)\ln(\Lambda/\mu)}\ . \tag{3.14}$$

G_μ and the scale μ in Eq. (3.14) are not independent. A change in μ can be compensated by adjusting G_μ such that $1/G_\mu-\frac{1}{6}\ln(\mu)=$const. This "constant" is arbitrary and plays the role of C in Eq. (3.6). In Figs. 10(a) and 10(b) we show bound-state energies in the presence of the modified asymptotic counterterm [Eq. (3.13)] for two particular choices of the *constant* (crosses). One finds that by adjusting the constant a much wider range of possible eigenvalues can be covered, compared to the situation with the box counterterm.

In the cases $|J_z|=1$ the asymptotic kernel is a function of longitudinal and transverse momenta. Therefore, the corresponding asymptotic counterterm would also be a function of both the longitudinal and transverse momenta. According to power counting, however, transverse divergences are removable by counterterms that depend only on longitudinal momenta, and transverse momentum dependence in counterterms should not be necessary. Therefore, we do not consider further the asymptotic counterterms.

IV. CALCULATIONS INCLUDING SELF-ENERGY CORRECTIONS

We now discuss effects of introducing the self-energy term $T_{\rm SE}$ given in Eq. (2.33). Note that in the bound-state problem the self-energy is a function of the bound-state energy M^2. The most severe ultraviolet divergence in $(T_{\rm SE})_{(M^2)}$ is a quadratical divergence. We eliminate this divergence by subtracting at the threshold $M^2=M_0^2\equiv(m_F^2+k^2)/[x(1-x)]$:

$$(T_{\rm SE})_{(M^2)}\to(T_{\rm SE})_{(M^2)}-(T_{\rm SE})_{(M_0^2)}$$
$$\equiv g^2(M^2-M_0^2)\sigma_{(M^2)}\ . \tag{4.1}$$

$\sigma_{(M^2)}$ is still logarithmically divergent. In terms of a cutoff Λ for the $d^2q^\perp$ integration in (2.3), one finds

$$\sigma_{(M^2)}=-\pi\int_0^1 dy\,(1-y)\left[\ln\frac{\Lambda^2+A_a}{A_a}+\ln\frac{\Lambda^2+A_b}{A_b}\right]$$
$$+\frac{(4m_f^2-m_B^2)\pi}{M^2-M_0^2}\int dy\left[\frac{1}{x}\left[\ln\frac{\Lambda^2+A_f}{A_f}-\ln\frac{\Lambda^2+A_a}{A_a}\right]+\frac{1}{1-x}\left[\ln\frac{\Lambda^2+A_f}{A_f}-\ln\frac{\Lambda^2+A_b}{A_b}\right]\right] \tag{4.2}$$

with

$$A_f = y m_B^2 + (1-y)^2 m_f^2 , \tag{4.3a}$$

$$A_a = A_f - y(1-y)x(M^2 - M_0^2) , \tag{4.3b}$$

$$A_b = A_f - y(1-y)(1-x)(M^2 - M_0^2) . \tag{4.3c}$$

The logarithmically divergent piece of (4.2) corresponds to wave-function renormalization of the two fermion lines. One finds

$$\sigma_{\text{log div part}} = \left[\frac{\partial T_{\text{SE}}}{\partial M^2} \right]_{\text{log div}}$$
$$= -(2\pi) \int dy (1-y) \ln \frac{\Lambda^2 + A_f}{A_f}$$
$$\equiv -W(\Lambda) . \tag{4.4}$$

One can absorb this divergence into a new definition of the coupling constant. The way this works is as follows. After the subtraction (4.1), but ignoring all boson-exchange counterterms, Eq. (2.31) becomes

$$(M^2 - M_0^2)\Psi_2^{\sigma_1\sigma_2}(\mathbf{k},x) = \frac{\alpha}{4\pi^2} X_{\text{BE}} + \frac{\alpha}{4\pi^2}(M^2 - M_0^2) \times \sigma_{(M^2)} \Psi_2^{\sigma_1\sigma_2}(\mathbf{k},x) , \tag{4.5}$$

where X_{BE} stands for the term with the kernel K in (2.31). One can now rearrange terms in Eq. (4.5) giving (we suppress all spin indices)

$$(M^2 - M_0^2)\left[1 + \frac{\alpha}{4\pi^2} W(\Lambda)\right]\Psi = \frac{\alpha}{4\pi^2} X_{\text{BE}} + \frac{\alpha}{4\pi^2}(M^2 - M_0^2) \times [\sigma + W(\Lambda)]\Psi . \tag{4.6}$$

The RHS of (4.6) is not finite. One must still deal with the divergent piece W on the LHS of the equation. Define

$$\alpha_R = \frac{\alpha}{1 + (\alpha/4\pi^2) W(\Lambda)} \tag{4.7}$$

then one can trade a Λ-dependent bare coupling α in favor of a finite renormalized coupling α_R. Equation (4.6) then becomes

$$(M^2 - M_0^2)\Psi = (\alpha_R/4\pi^2) X_{\text{BE}} + (\alpha_R/4\pi^2)(M^2 - M_0^2)[\sigma + W(\Lambda)]\Psi \tag{4.8}$$

or

$$(M^2 - M_0^2)\Psi = \frac{\alpha_R/4\pi^2}{1 - (\alpha_R/4\pi^2)[\sigma_{(M^2)} + W(\Lambda)]} X_{\text{BE}} . \tag{4.9}$$

One sees that the form of Eq. (4.9) is identical to what was solved in the previous section (where we ignored all counterterms) with α replaced by $\alpha_R/[1-(\alpha_R/4\pi^2)(\sigma + W)]$. One should note that σ is a function of x and k, and therefore effectively changes the kernel. In lowest-order Tamm-Dancoff the divergent parts of T_{SE} can hence be absorbed into a renormalized mass and coupling. It is, however, not clear whether this method will work in higher orders and this issue should be investigated further.

Before proceeding let us consider Eq. (4.7) more carefully. Inverting the equation one has

$$\alpha(\Lambda) = \frac{\alpha_R}{1 - (\alpha_R/4\pi^2) W(\Lambda)} . \tag{4.10}$$

One sees that for every value of α_R other than $\alpha_R = 0$ there will be a cutoff Λ at which the denominator in (4.10) vanishes and α becomes infinite. Beyond that point α would be imaginary. This is just a manifestation of "triviality" in this model. The only way the theory can be sensible for an arbitrary large cutoff $\Lambda \to \infty$ is when $\alpha_R \to 0$. In practice, this means that for fixed cutoff there will be an upper bound on α_R. Taking this bound to be the point at which the denominator in (4.10) vanishes, one ends up with the triviality curve of Fig. 11. The curve is shown for $m_B = 0.25$; however, we have found that m_B dependence is very mild. In solving our bound-state equations we will always have to work with Λ's and α_R's below the triviality curve. If the cutoff is too large we may be forced into a theory with very small α_R so that no bound states exist. It should be noted, however, that although the triviality curve is fairly insensitive to the boson mass m_B, the number of bound states does depend on its value. The smaller m_B the more bound states one has for given Λ and α_R. Our choices for m_B, α_R, and Λ were made with all these constraints in mind.

In Figs. 12–14 we show results for bound-state energies in the $J_z = 0$ and 1 sectors. These are to be compared with Figs. 5, 8, and 9 of the previous section where self-energy corrections were ignored. One finds again two bound states for $J_z = 0$ and one bound state for $J_z = 1$. Even after eliminating divergences coming from the self-

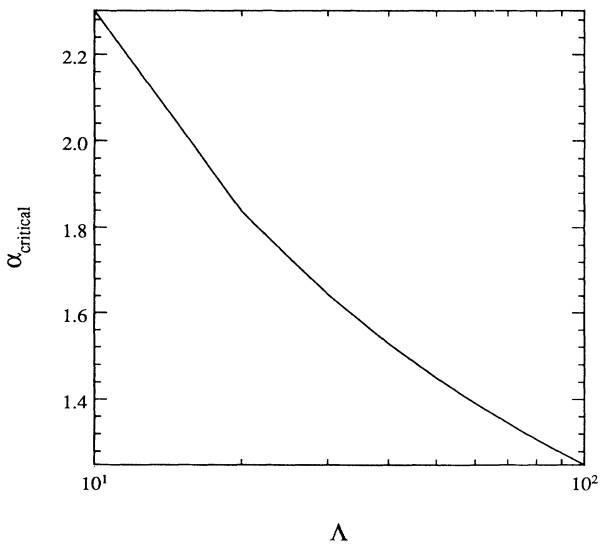

FIG. 11. The critical coupling vs the cutoff Λ for $m_B = 0.25$.

energy, that is, after carrying out a subtraction at $M^2=M_0^2$ and introducing a renormalized coupling, one still has the divergences appearing in the boson-exchange term. For the $(1-,2+)$ sector where the boson-exchange kernel has an attractive diverging piece, one sees that self-energy corrections have made the cutoff dependence more severe. This is because for large $|\kappa^\perp|\equiv k$, the effective coupling in Eq. (4.9),

$$\alpha_{\text{effective}}(k,x;M^2)=\frac{\alpha_R}{1-(\alpha_R/4\pi^2)(\sigma_{(k,x;M^2)}+W)} \tag{4.11}$$

is larger than α_R and this enhances sensitivity to large-k behavior. In those channels in which the boson-exchange

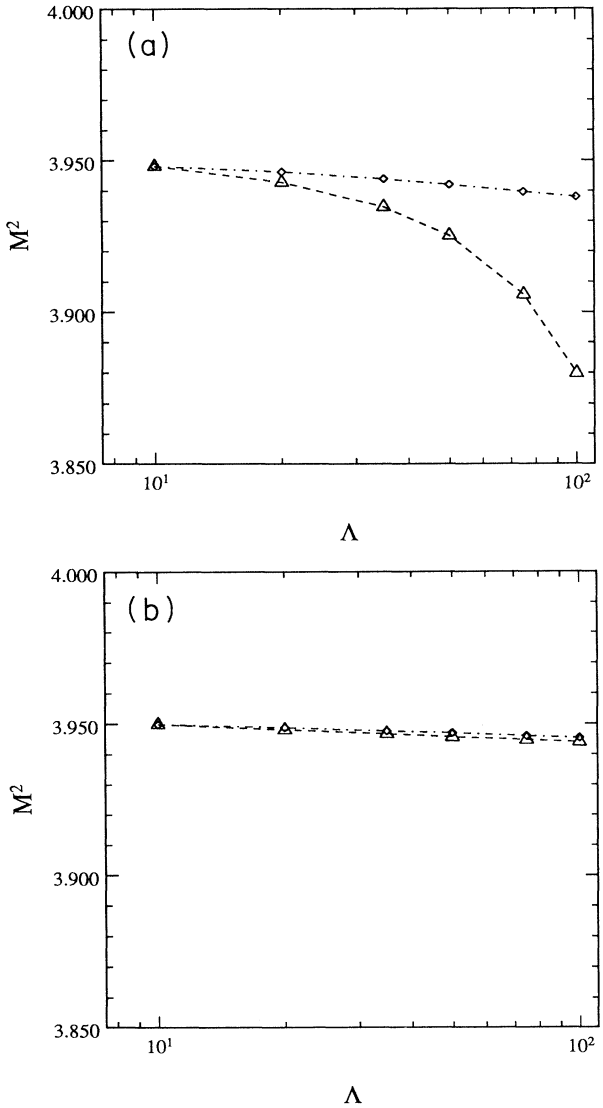

FIG. 12. (a) The bound-state mass M^2 vs the cutoff Λ with self-energy correction in the helicity-zero sector for $m_B=0.25$ and $\alpha_R=1.184$ for the $(1-,2+)$ state. No boson-exchange counterterm, dashed (triangle); one box counterterm ($C=2.3026$), dot-dashed (diamond). (b) Same as in (a) but for the $(1+,2-)$ state.

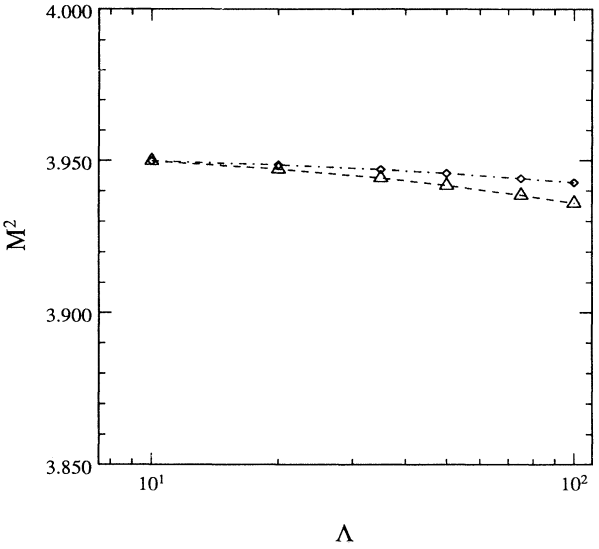

FIG. 13. The bound-state mass M^2 vs the cutoff Λ with self-energy correction in the helicity-one sector for $m_B=0.25$ and $\alpha_R=1.184$. No boson-exchange counterterm, dashed (triangle); one box counterterm ($C=2.3026$), dot-dashed (diamond).

divergence is repulsive the replacement of α by $\alpha_{\text{effective}}$ will deemphasize the large-k part of the wave function. The boson-exchange counterterms for the most part removes the cutoff dependence of the solutions, especially within the range of Λ allowed by triviality considerations. This will be demonstrated below.

In the previous section we discussed two ways to remove divergence coming from boson exchanges, the box counterterm and the asymptotic counterterm. We have combined self-energy corrections and box CT by modifying Eq. (4.9),

$$(M^2-M_0^2)\Psi=\frac{\alpha_R/4\pi^2}{1-(\alpha_R/4\pi^2)[\sigma_{(M^2)}+W(\Lambda)]}\times[X_{\text{BE}}+B_{\text{CT}}]\ , \tag{4.12}$$

where B_{CT} in the square brackets incorporates the counterterm (3.6) in the appropriate spin channels and the x and k dependences in $\alpha_{\text{effective}}$. Note that $[X_{\text{BE}}+B_{\text{CT}}]$ is correct through order α_R^2 whereas we have kept all orders of α_R in the effective coupling $\alpha_{\text{effective}}$ of (4.11). In Figs. 12 (helicity zero) and 13 (helicity one) we show the results for the bound-state energies as a function of Λ (diamonds) and compare with the "no box CT" case (triangles). One sees that the box CT is able to modify significantly the high-momentum part of the problem and render things fairly insensitive to the cutoff. Finally, in Fig. 14 we demonstrate what happens when one has self-energy corrections plus the asymptotic CT for the helicity-zero bound states.

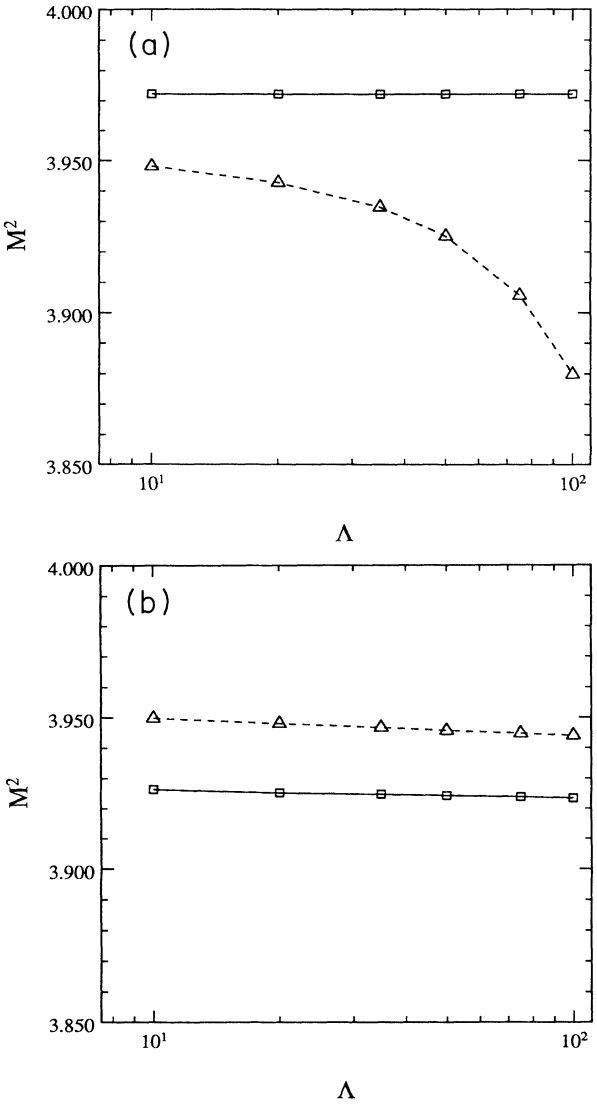

FIG. 14. (a) The bound-state mass M^2 vs the cutoff Λ with self-energy correction in the helicity-zero sector for $m_B=0.25$ and $\alpha_R=1.184$ for the $(1-,2+)$ state. No boson-exchange counterterm, dashed (triangle); asymptotic counterterm, solid (square). (b) Same as in (a) but for the $(1+,2-)$ state.

V. SUMMARY AND CONCLUSIONS

Attempts to solve relativistic Hamiltonians often result in equations containing divergences. One can regulate the divergences using cutoffs. The cutoffs violate Lorentz invariance. From practical considerations one is also forced to introduce particle truncation which, in turn, also spoil Lorentz invariance. One can try to renormalize the theory by introducing appropriate counterterms (nonlocal if necessary) to remove the divergences and also to recover the Lorentz symmetries. In the case of light-front field theory counterterms are, in general, nonlocal and noncovariant. Even though the spectrum of hadrons is of utmost interest light-front Hamiltonian of gauge theories is plagued with divergences arising from both small longitudinal momenta and large transverse momenta. To familiarize ourselves with the renormalization program we have initiated a study of the bound-state problem in the light-front Yukawa model where only the divergence arising from large transverse momenta causes trouble.

When one tries to choose a Hamiltonian in light-front field theory one is immediately faced with a novel issue. In equal-time theory one can either start from the canonical Hamiltonian or rely on power counting. Either way one can come up with a Hamiltonian with a finite number of terms. The situation is drastically different on the light-front because of the existence of two different dimensional variables x^- and $x^\perp$. The canonical Hamiltonian still has only a limited number of terms but if one relies solely on power counting an unlimited number of terms emerge. Nonlocal noncovariant terms can be generated also by the analysis of perturbation theory which is guaranteed to remove the divergence to a given order in perturbation theory.

In this work we have attempted the renormalization procedure both by adding noncanonical terms and by adding counterterms discovered in perturbation theory. In principle, one would like to remove the cutoff dependence for any coupling and any cutoff. However, in the present Yukawa model, because of triviality, we cannot go to large coupling for moderately large cutoffs. In order to have nontrivial physics a finite cutoff has to be retained. On the other hand, we show that within the present approximation we do get bound states and sensible low-energy physics that is insensitive to the cutoff. The general analysis has indicated that the finite part of the counterterm is an arbitrary function and not just a constant. In this work we studied the consequence of just an arbitrary constant. If we were to add an arbitrary function we would need a continuous set of conditions to fix this function. In the Yukawa model this will inevitably take us to a consideration of the two-fermion scattering problem which is an important project that needs to be carried out in the future. Imposing rotational symmetry on scattering amplitudes should place severe constraints on the counterterms. Will one then also obtain a rotationally symmetric bound-state spectrum or are additional counterterms required? Alternatively, if one works in a regime in parameter space that exhibits a large number of bound states, does fixing rotational invariance in the low-lying states ensure correct degeneracies in the higher levels? We note, on the other hand, that even if the invariant masses of low-lying bound states cannot be predicted, but are instead input to fix counterterms, one would nevertheless end up with knowledge about wave functions and hence gain a lot of information about the structure of bound states. Clearly, however, a lot more work is necessary before light-front field theory is established as a viable method for relativistic bound state problems.

We view the present work as a first step in confronting the problem of renormalization of light-front Hamiltonian field theories. It is of interest to apply similar methods in theories with asymptotic freedom after suitable modifications to the Tamm-Dancoff truncations.

ACKNOWLEDGMENTS

We are indebted to Robert J. Perry for many enlightening discussions. We also acknowledge helpful conversations with Charlotte Elster and Dave Wasson. We thank John E. Davis for making available his plotting package EZPLOT. We thank the Aspen Center for Physics for hospitality. This work was supported in part by the National Science Foundation under Grant Nos. PHY-8719526 and PHY-8858250 and by the Department of Energy and by a grant from Cray Research, Inc. S.G. was supported in part by Komitet Badań Naukowych under Grant No. KBN 2 0273 91 01. The computational support of the Ohio Supercomputer Center is also gratefully acknowledged.

APPENDIX A: POWER COUNTING, POSSIBLE INTERACTIONS, AND THE STRUCTURE OF DIVERGENCES

Power counting can be utilized to construct possible terms in the Hamiltonian. First we outline this procedure in equal-time theory. We compare and contrast the situations in equal-time and light-front field theories. As an example consider the Yukawa theory of fermions and scalar bosons. Let us denote the scalar field by ϕ and the fermion field by ψ. Let x be the dimensional variable. Then the canonical dimensions are $m=1/x$, $\partial=1/x$, $\phi=1/x$, $\psi=1/x^{3/2}$. The canonical dimensions of the Hamiltonian H and the Hamiltonian density $\mathcal{H}$ are $1/x$ and $1/x^4$, respectively. Then possible terms in $\mathcal{H}$ according to the power counting are $m^2\phi^2$, $(\partial\phi/\partial t)^2$, $\partial\phi\cdot\partial\phi$, $m\bar{\psi}\psi$, $\bar{\psi}\alpha\cdot\partial\psi$, $\bar{\psi}\phi\psi$, $a_1\phi$, $a_3\phi^3$, and ϕ^4. Here a_1 and a_3 have canonical dimensions $1/x^3$ and $1/x$, respectively. Note that this exhausts the possibilities in $3+1$ dimensions. When we analyze the divergences we find that the counterterms required are also of the same form as suggested by power counting.

The situation is remarkably different in light-front field theory. It was observed that in light-front coordinates one has two dimensional variables x^- and $x^\perp$ [23]. One also has the inverse derivative operator $1/\partial^+$ which appears even in the free-fermion Hamiltonian. Recall that ψ^+, not ψ, is the true fermion dynamical variable in light-front theory. The various canonical dimensions are $\partial^+=1/x^-$, $\partial^\perp=1/x^\perp$, $\phi=1/x^\perp$, $\psi^+=1/(x^\perp\sqrt{x^-})$, $H=x^-/(x^\perp)^2$, $\mathcal{H}=1/(x^\perp)^4$. Terms in $\mathcal{H}$ allowed by power counting are $a_1\phi$, $a_3\phi^3$, ϕ^4, $m^2\phi^2$, $\partial^\perp\phi\cdot\partial^\perp\phi$, $m^2(\psi^+)^\dagger(1/\partial^+)\psi^+$, $(\psi^+)^\dagger[(\partial^\perp)^2/(\partial^+)]\psi^+$, $m(\psi^+)^\dagger(1/\partial^+)\psi^+\phi$, $(\psi^+)^\dagger\gamma^\perp\cdot\partial^\perp(1/\partial^+)\psi^+\phi$, $(\psi^+)^\dagger\phi(1/\partial^+)\phi\psi^+$, ... Here a_1 and a_3 have canonical dimensions $1/(x^\perp)^3$ and $1/x^\perp$, respectively. We have listed all the terms that appear in the canonical Hamiltonian and the ellipsis indicates terms that are allowed by power counting but do not appear in the canonical Hamiltonian. An example of such a term is a four-fermion interaction of the form $(\psi^+)^\dagger\Gamma\psi^+[1/(\partial^+)^2](\psi^+)^\dagger\Gamma\psi^+$ where Γ is a Dirac matrix.

The divergences in light-front theory are, in general, nonlocal in sharp contrast to the equal-time case. Recall the relationship between energy and momentum in equal-time theory, $E=\sqrt{\mathbf{k}^2+m^2}$. Thus, energy divergences occur when momenta get very large and hence the divergence has an entirely local structure. This situation is to be contrasted with the light-front case where $k^-=(\kappa^{\perp 2}+m^2)/k^+$. Because the energy factorizes into k^+ and $\kappa^\perp$ the subtractions are not constants. That is, for example, when $\kappa^\perp$ gets very large the energy diverges no matter what k^+ is. Thus, in general, we get a divergent constant *multiplied by a function of* k^+. Similarly for the case when k^+ gets very small. In position space this translates into divergences at small $x^\perp$ being nonlocal in x^- and spread out over the light cone. Thus, the subtractions needed may not be of the same form as the terms appearing in the canonical Hamiltonian. One may require noncanonical nonlocal terms consistent with the power counting of the previous paragraph.

APPENDIX B: HIGH-LOW ANALYSIS

From a Fock-space point of view any relativistic bound-state problem in field theory is a twofold infinite-dimensional coupled channel problem. The state vector for any system can be expanded in terms of multiparticle amplitudes $\{\phi_n\}$ and there are, in principle, an infinite number of them coupled via the eigenvalue equation. In practice, one truncates this series and arrives at an equation for the *dominant amplitude*. The resulting equation, in general, contains a very complicated effective interaction. The single-particle momenta in this equation runs from zero all the way to the cutoff. Thus, there are still an infinite number of energy scales involved in the problem. All these different energy scales get coupled via the effective interaction. Our aim is to solve the theory in the low-energy domain. However, depending upon the nature of the effective interaction, if one simply solves the theory one usually finds that the low-energy observables show strong dependence on the high-energy cutoff. By introducing suitable counterterms one should renormalize the bound-state equation so that (a) the cutoff dependence is eliminated from the low-energy observables and (b) sufficient flexibility exist in the finite parts of the counterterms so that one is able to renormalize to some experimental input.

The basic ideas of the renormalization program can be illustrated with a simple example. Consider an eigenvalue equation of the form [24]

$$k\phi(k)-g\int_0^\Lambda dq\, V(k,q)\phi(q)=E\phi(k)\ . \tag{B1}$$

We introduce an intermediate scale L. L is assumed to be large compared to the low-energy eigenvalues and small compared to the high-momentum cutoff Λ. We divide the momentum space into two domains:

$$\begin{aligned} &0<k<L\text{: low region ,}\\ &L<k<\Lambda\text{: high region .}\end{aligned} \tag{B2}$$

We split the amplitude

$$\begin{aligned} &\phi(k)=\phi_L(k)\text{: } 0<k<L\ ,\\ &\phi(k)=\phi_H(k)\text{: } L<k<\Lambda\ .\end{aligned} \tag{B3}$$

Thus, we end up with a system of two coupled equations:

$$k\phi_L(k)-g\int_0^L dq\ V_{LL}(k,q)\phi_L(q) -g\int_L^\Lambda dq\ V_{LH}(k,q)\phi_H(q)=E\phi_L(k)\ , \tag{B4}$$

$$k\phi_H(k)-g\int_0^L dq\ V_{HL}(k,q)\phi_L(q) -g\int_L^\Lambda dq\ V_{HH}(k,q)\phi_H(q)=E\phi_H(k)\ . \tag{B5}$$

Now assume that

$$V_{LH}(k,q)=V_{HL}(k,q)=V_{HH}(k,q)=f\ . \tag{B6}$$

This assumption fails in many realistic field theories including the Yukawa model. It is nevertheless instructive first to discuss toy models where (B6) holds. To find the possible structure of counterterms, first we perform a perturbative analysis. Assuming g, the strength of the interaction, is very small one can ignore the second term in the interaction in Eq. (B5) and solve for $\phi(k)_H$ in terms of $\phi(k)_L$ and substitute back into Eq. (B4). Thus, we arrive at

$$k\phi_L(k)-g\int_0^L dq\ V_{LL}(k,q)\phi_L(q) -g^2f^2\ln\frac{\Lambda}{L}\int_0^L dq\ \phi_L(q)=E\phi_L(k)\ . \tag{B7}$$

Thus, to order g^2 we need a counterterm of the form

$$g^2f^2\ln\Lambda\int_0^\Lambda dq\ \phi(q)\ . \tag{B8}$$

Once we have determined the generic form of the counterterm we abandon perturbative analysis and start from a modified equation:

$$k\phi(k)-g\int_0^\Lambda dq\ V(k,q)\phi(q)+G_\Lambda\int_0^\Lambda dq\ \phi(q)=E\phi(k)\ . \tag{B9}$$

Again, performing the high-low separation we have

$$k\phi_L(k)-g\int_0^L dq\ V_{LL}(k,q)\phi_L(q)-g\int_L^\Lambda dq\ V_{LH}(k,q)\phi_H(q)+G_\Lambda\int_0^L dq\ \phi_L(q)+G_\Lambda\int_L^\Lambda dq\ \phi_H(q)=E\phi_L(k)\ , \tag{B10}$$

and

$$k\phi_H(k)-g\int_0^L dq\ V_{HL}(k,q)\phi_L(q)-g\int_L^\Lambda dq\ V_{HH}(k,q)\phi_H(q)+G_\Lambda\int_0^L dq\ \phi_L(q)+G_\Lambda\int_L^\Lambda dq\ \phi_H(q)=E\phi_H(k)\ . \tag{B11}$$

Solving for ϕ_H exactly from Eq. (B11) we have

$$\int_L^\Lambda dq\ \phi_H(q)=\frac{(gf-G_\Lambda)\ln(\Lambda/L)}{1-(gf-G_\Lambda)\ln(\Lambda/L)}\int_0^L dq\ \phi_L(q)\ . \tag{B12}$$

Substituting back into Eq. (B11) we find

$$k\phi_L(k)-g\int_0^L dq\,[V_{LL}(k,q)-f]\phi_L(q) -\frac{gf-G_\Lambda}{1-(gf-G_\Lambda)\ln(\Lambda/L)}\int_0^L dq\ \phi_L(q)=E\phi_L(k)\ . \tag{B13}$$

If we now set

$$gf-G_\Lambda=A_\Lambda\ , \tag{B14}$$

we find Eq. (B13) to be independent of Λ by requiring

$$\frac{1-A_\Lambda\ln(\Lambda/L)}{A_\Lambda}=\frac{1}{A_L}\ , \tag{B15}$$

thus

$$\frac{1}{A_\Lambda}-\ln\Lambda=\frac{1}{A_L}-\ln L=C=\frac{1}{A_\mu}-\ln\mu\ , \tag{B16}$$

and

$$G_\Lambda=gf-\frac{A_\mu}{1+A_\mu\ln(\Lambda/\mu)}\ . \tag{B17}$$

The renormalized equation is therefore

$$k\phi(k)-g\int_0^\Lambda dq\,[V(k,q)-f]\phi(q) -\frac{A_\mu}{1+A_\mu\ln(\Lambda/\mu)}\int_0^\Lambda dq\ \phi(q)=E\phi(k)\ . \tag{B18}$$

We have renormalized the original equation in the sense that the low-energy eigenvalue E is independent of the high-energy cutoff and we have an arbitrary parameter C which can be adjusted to fit the ground-state energy level.

One can motivate both the asymptotic counterterm and one-box counterterm of Secs. III and IV as different choices in our analysis. Our starting point is Eq. (B18). For a fixed μ we are free to choose A_μ at will. The simple asymptotic counterterm corresponds to $A_\mu=0$. However, subtracting the asymptotic behavior of the kernel with the term gf causes the wave function to fall off more rapidly than it would otherwise at large q. As a result the $[A_\mu/(1+A_\mu\ln\Lambda/\mu)]\int\phi\,dq$ in Eq. (B18) is finite, and this term can be retained as an arbitrary adjustable finite counterterm.

The perturbative counterterms correspond to $A_\mu=gf$ then expanding in $g\ln\Lambda/\mu$. Equation (B18) then becomes

$$k\phi(k)-g\int_0^\Lambda dq\,[V(k,q)-f]\phi(q) -gf\sum_{n=0}^{\infty}(-gf\ln\Lambda/\mu)^n\int_0^\Lambda dq\ \phi(q)=E\ . \tag{B19}$$

Keeping the first two terms in the expansion we get the so-called "box counterterm"

$$k\phi(k)-g\int_0^\Lambda dq\ V(k,q)\phi(q) +g^2f^2\ln\Lambda/\mu\int_0^\Lambda dq\ \phi(q)=E\ . \tag{B20}$$

Note that the box counterterm contains f^2 indicating that it involves the kernel at high momentum twice. We see this in the graphical view of the box counterterm shown in Fig. 7. $\ln\mu$ remains a free parameter and in the Yukawa model calculation we let $C=-\ln\mu$.

Ideally, one would like to carry out the nonperturbative renormalization program rigorously in the sense that the cutoff independence is achieved for any value of the coupling constant and any value of the cutoff. In practical cases, either we may not have the luxury to go to very large cutoff or the analysis itself may get too complicated. For example, the assumption given by Eq. (B6) was essential for summing up the series. In reality V_{HH} may differ from V_{LH}.

Next we consider simplified two-variable problems that are more closely related to the equation and approximations used in the paper. The form of the asymptotic counterterm that we use can be understood by considering the equation

$$\frac{k}{x(1-x)}\phi(k,x)-g\int_0^\Lambda dq\int_0^1 dy\,K(k,q)\phi(q,y) =E\phi(k,x)\ . \quad \text{(B21)}$$

This problem contains only an x dependence associated with the free energy, and no x dependence in the kernel. Equation (B21) is easily solved using the high-low analysis used above and we find

$$k\phi(kx)-g\int_0^\Lambda dq\int_0^1 dy\,[K(k,q)-f]\phi(q,y) -\frac{A_\mu}{1+(1/6)A_\mu\ln\Lambda/\mu}\int_0^\Lambda dq\int_0^1 dy\,\phi(q,y)=E\phi(k,x)\ . \quad \text{(B22)}$$

The factor of $\frac{1}{6}$ comes from the integral $\int_0^1 dx\,x(1-x)$. This result motivates our choice for G_Λ in Eq. (3.14).

We now return to the box counterterm in the two-variable problem. The kernel appearing in the bound-state problem in the Yukawa model exhibits a very rich structure. To familiarize ourselves with the renormalization problems associated with such complicated kernels we consider the equation

$$\frac{k}{x(1-x)}\phi(k,x)-g\int_0^\Lambda dq\int_0^1 dy\,V(k,x;q,y)\phi(q,y) =E\phi(k,x)\ . \quad \text{(B23)}$$

Doing a high-low analysis we arrive at

$$\frac{k}{x(1-x)}\phi_L(k,x)-g\int_0^L dq\int_0^1 dy\,V_{LL}(k,x;q,y)\phi_L(q,y)-g\int_L^\Lambda dq\int_0^1 dy\,V_{LH}(k,x;q,y)\phi_H(q,y)=E\phi_L(k,x)\ , \quad \text{(B24)}$$

$$\frac{k}{x(1-x)}\phi_H(k,x)-g\int_0^L dq\int_0^1 dy\,V_{HL}(k,x;q,y)\phi_L(q,y)-g\int_L^\Lambda dq\int_0^1 dy\,V_{HH}(k,x;q,y)\phi_H(q,y)=E\phi_H(k,x)\ . \quad \text{(B25)}$$

Assume

$$V_{LH}(k,x;q,y)=V_{HL}(k,x;q,y)=f(x,y)\ , \quad \text{(B26)}$$

where $f(x,y)$ is the analogue of $f(x,y)$ in Eq. (3.6).

Note that this assumption which is less restrictive than Eq. (B6) is indeed satisfied by the Kernel in the bound-state problem of the Yukawa model. We will analyze Eq. (B23) only to the lowest order in the perturbation theory where knowledge of $V_{HH}(k,x;q,y)$ is not required.

From Eq. (B25) to lowest order in perturbation theory,

$$\phi_H(q,y)=g\frac{y(1-y)}{q}\int_0^L dp\int_0^1 dz\,h(y,z)\phi_L(p,z)\ . \quad \text{(B27)}$$

Substituting back into Eq. (B24) we have

$$\frac{k}{x(1-x)}\phi_L(k,x)-g\int_0^L dq\int_0^1 dy V_{LL}(k,x;q,y)\phi_L(q,y) -g^2\ln\frac{\Lambda}{L}\int_0^L dq\int_0^1 dz\int_0^1 dy\,f(x,z)z(1-z)f(z,y)\phi_L(q,y)=E\phi_L(k,x)\ , \quad \text{(B28)}$$

and this result motivates the "box counterterm" $V^{\mathrm{BCT}}(x,y)$ in Eq. (3.6). To order g^2 we have found the box counterterm

$$\int_0^\Lambda dq\int_0^1 dy\,K(x,y)\phi(q,y)\ , \quad \text{(B29)}$$

where

$$K(x,y)=g^2\ln\frac{\Lambda}{L}\int_0^1 dz\,f(x,z)z(1-z)f(z,y)\ . \quad \text{(B30)}$$

Thus, perturbation theory indicates that a possible general form of the counterterm is

$$G_\Lambda\int_0^1 dy\int_0^\Lambda dq\,F(x,y)\phi(q,y)\ . \quad \text{(B31)}$$

The unknown function $F(x,y)$ is to be determined by a *nonperturbative* analysis. This problem can be solved exactly for some specific assumption about $V_{HH}(k,x;q,y)$.

APPENDIX C: EXPLICIT FORM OF THE KERNELS

The kernels are as follows.

$J_z=0$:

$$V(k,x;q,y;M^2)^{1\pm,1\pm}=\left[m_F^2\left[\frac{1}{x}+\frac{1}{y}\right]\left[\frac{1}{1-x}+\frac{1}{1-y}\right]\mp\left[\frac{k^2}{x(1-x)}+\frac{q^2}{y(1-y)}\right]\right]I_2 \pm kq\left[\frac{1}{y(1-x)}+\frac{1}{x(1-y)}\right]I_1 , \tag{C1}$$

$$V(k,x;q,y;M^2)^{1\pm,2\mp}=m_F\left[\frac{1}{x}+\frac{1}{y}\right]\left[\frac{-k}{1-x}I_1+\frac{q}{1-y}I_2\right]\pm m_F\left[\frac{1}{1-x}+\frac{1}{1-y}\right]\left[\frac{-k}{x}I_1+\frac{q}{y}I_2\right] , \tag{C2}$$

$$V(k,x;q,y;M^2)^{2\mp,1\pm}=m_F\left[\frac{1}{x}+\frac{1}{y}\right]\left[\frac{k}{1-x}I_2-\frac{q}{1-y}I_1\right]\mp m_F\left[\frac{1}{1-x}+\frac{1}{1-y}\right]\left[\frac{-k}{x}I_2+\frac{q}{y}I_1\right] , \tag{C3}$$

$$V(k,x;q,y;M^2)^{2\mp,2\mp}=\left[m_F^2\left[\frac{1}{x}+\frac{1}{y}\right]\left[\frac{1}{1-x}+\frac{1}{1-y}\right]\mp\left[\frac{k^2}{x(1-x)}+\frac{q^2}{y(1-y)}\right]\right]I_1 \pm kq\left[\frac{1}{y(1-x)}+\frac{1}{x(1-y)}\right]I_2 . \tag{C4}$$

$J_z=1$:

$$V(k,x;q,y;M^2)^{\uparrow\uparrow,\uparrow\uparrow}=m_F^2\left[\frac{1}{x}+\frac{1}{y}\right]\left[\frac{1}{1-x}+\frac{1}{1-y}\right]I_1 , \tag{C5}$$

$$V(k,x;q,y;M^2)^{\uparrow\uparrow,\uparrow\downarrow}=m_F\left[\frac{1}{x}+\frac{1}{y}\right]\left[\frac{-k}{1-x}I_2+\frac{q}{1-y}I_1\right] , \tag{C6}$$

$$V(k,x;q,y;M^2)^{\uparrow\uparrow,\downarrow\uparrow}=m_F\left[\frac{1}{1-x}+\frac{1}{1-y}\right]\left[\frac{k}{x}I_2-\frac{q}{y}I_1\right] , \tag{C7}$$

$$V(k,x;q,y;M^2)^{\uparrow\uparrow,\downarrow\downarrow}=\frac{-k^2}{x(1-x)}I_3-\frac{q^2}{y(1-y)}I_1 +kq\left[\frac{1}{y(1-x)}+\frac{1}{x(1-y)}\right]I_2 , \tag{C8}$$

$$V(k,x;q,y;M^2)^{\uparrow\downarrow,\uparrow\uparrow}=m_F\left[\frac{1}{x}+\frac{1}{y}\right]\left[\frac{k}{1-x}I_1-\frac{q}{1-y}I_2\right] , \tag{C9}$$

$$V(k,x;q,y;M^2)^{\uparrow\downarrow,\uparrow\downarrow}=m_F^2\left[\frac{1}{x}+\frac{1}{y}\right]\left[\frac{1}{1-x}+\frac{1}{1-y}\right]I_2 , \tag{C10}$$

$$V(k,x;q,y;M^2)^{\uparrow\downarrow,\downarrow\uparrow}=\left[\frac{k^2}{x(1-x)}+\frac{q^2}{y(1-y)}\right]I_2 -kq\left[\frac{1}{y(1-x)}I_1+\frac{1}{x(1-y)}I_3\right] , \tag{C11}$$

$$V(k,x;q,y;M^2)^{\uparrow\downarrow,\downarrow\downarrow}=m_F\left[\frac{1}{1-x}+\frac{1}{1-y}\right]\left[\frac{k}{x}I_3-\frac{q}{y}I_2\right] , \tag{C12}$$

$$V(k,x;q,y;M^2)^{\downarrow\uparrow,\uparrow\uparrow}=m_F\left[\frac{1}{1-x}+\frac{1}{1-y}\right]\left[\frac{-k}{x}I_1+\frac{q}{y}I_2\right] , \tag{C13}$$

$$V(k,x;q,y;M^2)^{\downarrow\uparrow,\uparrow\downarrow}=\left[\frac{k^2}{x(1-x)}+\frac{q^2}{y(1-y)}\right]I_2 -kq\left[\frac{1}{y(1-x)}I_3+\frac{1}{x(1-y)}I_1\right] , \tag{C14}$$

$$V(k,x;q,y;M^2)^{\downarrow\uparrow,\downarrow\uparrow}=m_F^2\left[\frac{1}{x}+\frac{1}{y}\right]\left[\frac{1}{1-x}+\frac{1}{1-y}\right]I_2 , \tag{C15}$$

$$V(k,x;q,y;M^2)^{\downarrow\uparrow,\downarrow\downarrow} = m_F\left[\frac{1}{x}+\frac{1}{y}\right]\left[\frac{-k}{1-x}I_3+\frac{q}{1-y}I_2\right], \quad \text{(C16)}$$

$$V(k,x;q,y;M^2)^{\downarrow\downarrow,\uparrow\uparrow} = -\frac{k^2}{x(1-x)}I_1-\frac{q^2}{y(1-y)}I_3 + kq\left[\frac{1}{y(1-x)}+\frac{1}{x(1-y)}\right]I_2, \quad \text{(C17)}$$

$$V(k,x;q,y;M^2)^{\downarrow\downarrow,\uparrow\downarrow} = m_F\left[\frac{1}{1-x}+\frac{1}{1-y}\right]\left[\frac{-k}{x}I_2+\frac{q}{y}I_3\right], \quad \text{(C18)}$$

$$V(k,x;q,y;M^2)^{\downarrow\downarrow,\downarrow\uparrow} = m_F\left[\frac{1}{x}+\frac{1}{y}\right]\left[\frac{k}{1-x}I_2-\frac{q}{1-y}I_3\right], \quad \text{(C19)}$$

$$V(k,x;q,y;M^2)^{\downarrow\downarrow,\downarrow\downarrow} = m_F^2\left[\frac{1}{x}+\frac{1}{y}\right]\left[\frac{1}{1-x}+\frac{1}{1-y}\right]I_3 . \quad \text{(C20)}$$

The integral

$$I_n = \int_0^{2\pi} du \frac{\cos\{(n-1)u\}}{a+b\cos(u)} = -2\pi\frac{1}{\sqrt{a^2-b^2}}\left[|a|-\frac{\sqrt{a^2-b^2}}{b}\right]^{|n-1|}, \quad \text{(C21)}$$

where $b=2kq$ and [same as Eq. (2.36)]

$$a = |x-y|\left[M^2-\frac{1}{2}\left[\frac{m_F^2+k^2}{x(1-x)}+\frac{m_F^2+q^2}{y(1-y)}\right]\right] - m_B^2+2m_F^2-\frac{m_F^2+k^2}{2}\left[\frac{y}{x}+\frac{1-y}{1-x}\right] - \frac{m_F^2+q^2}{2}\left[\frac{x}{y}+\frac{1-x}{1-y}\right]. \quad \text{(C22)}$$

[1] H. A. Bethe and F. de Hoffman, *Mesons and Fields* (Row, Peterson, Evanston, 1955), Vol. II.

[2] E. M. Henley and W. Thirring, *Elementary Quantum Field Theory* (McGraw-Hill, New York, 1962).

[3] R. J. Perry, A. Harindranath, and K. G. Wilson, Phys. Rev. Lett. **65**, 2959 (1990).

[4] H. C. Pauli and S. J. Brodsky, Phys. Rev. D **32**, 1993 (1985); **32**, 2001 (1985). Also see A. C. Tang, S. J. Brodsky, and H. C. Pauli, *ibid.* **44**, 1842 (1991); S. J. Brodsky and H. C. Pauli, in *Recent Aspect of Quantum Fields,* edited by H. Mitter and H. Gausterer, Lecture Notes in Physics Vol. 396 (Springer-Verlag, Berlin, 1991), and references therein.

[5] An extensive list of references on light-front physics (light.tex) is available via anonymous file transfer protocol (ftp) from public.mps.ohio-state.edu under the subdirectory tmp/infolight. See also S. Brodsky, H. C. Pauli, G. McCarter, and S. Pinsky, Particle World (to be published).

[6] K. G. Wilson, Phys. Rev. **140**, B445 (1965).

[7] K. G. Wilson, Phys. Rev. D **2**, 1438 (1970).

[8] St. Głazek and R. J. Perry, Phys. Rev. D **45**, 3734 (1992).

[9] A. C. Tang, SLAC Report No. 351, 1990 (unpublished).

[10] R. J. Perry and A. Harindranath, Phys. Rev. D **43**, 4051 (1991).

[11] A. Harindranath, R. J. Perry, and J. Shigemitsu, Phys. Rev. D **46**, 4580 (1992).

[12] M. Burkhardt and A. Langnau, Phys. Rev. D **44**, 3857 (1991).

[13] St. Głazek and R. J. Perry, Phys. Rev. D **45**, 3740 (1992); D. Mustaki and S. Pinsky, *ibid.* **45**, 3775 (1992).

[14] G. Feldman, T. Fulton, and J. Townsend, Phys. Rev. D **7**, 1814 (1973); P. Danielewicz and J. M. Namyslowski, Phys. Lett. **81B**, 110 (1979); L. Müller, Il Nuovo Cimento A **75**, 39 (1983); M. Sawicki, Phys. Rev. D **32**, 2666 (1985); **33**, 1103 (1986); C.-R. Ji and R. J. Furnstahl, Phys. Lett. **167B**, 11 (1986); C.-R. Ji, *ibid.* **167B**, 16 (1986).

[15] St. Głazek, Acta Phys. Pol. B **15**, 889 (1984).

[16] M. Krautgärtner, H. C. Pauli, and F. Wölz, Phys. Rev. D **45**, 3755 (1992).

[17] P. M. Wort, Phys. Rev. D **47**, 608 (1993).

[18] K. G. Wilson, in *New Pathways in High Energy Physics,* edited by A. Perlmutter (Plenum, New York, 1976), Vol. II, pp. 243–264.

[19] T. D. Lee, Phys. Rev. **95**, 1329 (1954).

[20] R. H. Dalitz and F. J. Dyson, Phys. Rev. **99**, 301 (1955).

[21] V. P. Silin, I. E. Tamm, and V. Ia. Fainberg, Zh. Eksp. Teor. Fiz. **29**, 6 (1956) [Sov. Phys. JETP **2**, 3 (1956)].

[22] B. T. Smith *et al.*, *Matrix Eigensystem Routines—EISPACK Guide* (Springer-Verlag, New York, 1983).

[23] K. G. Wilson, talk given at the Aspen Center for Physics, 1991 (unpublished). A videotape of this lecture is available from S. Pinsky.

[24] Similar equations have been studied by C. Thorn, Phys. Rev. D **19**, 639 (1979); R. Jackiw, in *M. A. Beg Memorial Volume,* edited by A. Ali and P. Hoodbhoy (World Scientific, Singapore, 1991); S. Pinsky, in QCD and High Energy Hadronic Interactions, Proceedings of the XXVII Rencontres de Moriond, 1992 (unpublished).